Correlating the Asphalt-Binder MSCR Test Results to the HMA Hamburg (HWTT) and Field Rutting Performance

Lubinda F. Walubita[1], Meng Ling[1*], Lorena M. Rico Pianeta[2], Luis Fuentes[2], Julius J. Komba[3], & Gamal M. Mabrouk[4]

Abstract: Asphalt-binder is one of the key constitutive components of hot-mix asphalt (HMA) that considerably affects its rutting performance. In particular, the high-temperature rheological properties measured from the Multiple Stress Creep and Recovery (MSCR) test are critical in quantifying the HMA rutting resistance. In this study, the Texas flexible pavements and overlays database (the Texas Data Storage System [DSS]) was used as the data source to investigate the effect of asphalt-binder high-temperature rheological properties on the HMA rutting resistance. The methodology of this study was based on correlating the results of the MSCR test and the Hamburg Wheel Tracking Test (HWTT) to HMA field rutting performance. The data matrix for this study included asphalt-binder (PG 64-22) from three different sources, three Texas widely used HMA mixes (fine gradation to coarse gradation), and five in-service highway test sections constructed using the same asphalt-binders and HMA mixes. In general, the MSCR non-recoverable creep compliance parameter, J_{nrdiff}, showed fairly strong correlations with the HMA rutting performance in the laboratory and field. The percent recovery parameter (R), on the other hand, exhibited the potential to ascertain and quantify the modifiers presence in the asphalt-binders. Furthermore, the test results indicated that material source/supplier has an impact on the rheological properties of the asphalt-binders with the same PG. Overall, the use of the MSCR

test to quantify the asphalt-binder high-temperature rheological properties indicated the potential to compliment the laboratory HWTT test for assessing the field HMA rutting performance in terms of the effects of asphalt-binder.

Key words: Asphalt-binder rheology; Hot-mix asphalt (HMA); Rutting; Multiple Stress Creep Recovery (MSCR); Hamburg Wheel Tracking Test (HWTT); Field rutting performance

---

*Corresponding Author | mengling@tamu.edu

[1]Texas A&M Transportation Institute (TTI), The Texas A&M University System, College Station, TX, USA

[2]Civil and Environmental Engineering Department, Universidad del Norte, Barranquilla, Colombia

[3]Council for Scientific and Industrial Research (CSIR) | University of Pretoria, South Africa

[4]Department of Civil and Environmental Engineering, University of Texas at San Antonio, San Antonio, TX, USA.

INTRODUCTION

Rutting is defined as longitudinal depressions on the pavement surface along the wheel path [1-8]. It is usually caused by consolidation and plastic deformation of any or all the pavement layers from surface to subgrade. Pavement rutting can be attributed to different factors such as high traffic loading, slow-speed vehicle loading, elevated temperatures, poor structural design, improper material selection/usage, poor HMA mix-designs, poor construction, and insufficient drainage [9–12]. Previous studies have shown that asphalt-binders play a critical role in the HMA performance, including rutting resistance [7,13–15]. The asphalt-binder component is responsible for the viscoelastic behavior of the HMA and has a direct influence on the HMA performance, especially in high-temperature environments, as asphalt-binder stiffness generally decreases, which makes the HMA more prone to rutting.

Over the years, conventional/basic test methods including penetration, softening point, and Saybolt-Furol viscosity have been explored to characterize and quantify the high-temperature rheological characteristics of asphalt-binders relative to HMA rutting performance [15-23]. Although relatively simple to perform, these tests are empirical in nature and not directly performance related [19,23]. From a technical perspective, these shortcomings can be attributed to: (a) the use of a single test temperature, (b) the specimen loading condition, (c) the high variability among test results, (d) the inability to reasonably characterize the asphalt-binder with respect to the mix rutting resistance and overall pavement performance, and (e) the unreliability to adopt for new generation materials such as modified asphalt-binders [18–20,23–25].

The Superior Performing Asphalt Pavements (Superpave) binder specification parameter $G^*/\sin\delta$ (complex modulus G^* and phase angle δ) was then suggested to characterize, evaluate, and quantify the high-temperature rheological properties of asphalt-binders [26]. Although the G*/ sin δ has been widely used, some deficiencies and limitations have been identified, particularly in characterizing the high-temperature rheological properties of polymer modified asphalt-binders (PMB) [15,27].

To supplement the G*/ Sin δ parametric characterization, a new Superpave Performance Graded (PG) laboratory test protocol was developed by the Federal Highway Administration (FHWA) for quantifying the fundamental high-temperature properties of both modified and unmodified asphalt-binders, namely the Multiple Stress Creep and Recovery (MSCR) [28]. The MSCR is a test method designed to evaluate the elastic response and the polymer modifier appearance [29]. The key output parameters from the MSCR test are the percent recovery (R) and non-recoverable creep compliance (J_{nr}) of asphalt-binders. Further, several studies have shown that J_{nr} is a good indicator of the asphalt-binder rutting resistance [15,30,31].

Like asphalt-binders, HMA mixes need to be evaluated and screened for rutting susceptibility during the mix-design phase. Over the years, several test methods have been developed to evaluate the rutting resistance of HMA mixes. The Marshall Stability and Hveem Stabilometer tests are among those originally developed to indirectly evaluate the rutting resistance of HMA. Since then, technological advancements have resulted in the development of devices specifically designed to assess the rutting resistance of HMA. The available HMA rutting tests include the Hamburg Wheel Tracking Tester (HWTT) [32,33], the Repeated Load Permanent Deformation (RLPD) test and the Superpave shear tester.

The literature review indicates that several studies have attempted to correlate asphalt-binder properties with the rutting resistance of HMA samples. For instance, Sybilski [34] and

Dreessen et al. [21] correlated the test results of penetration and softening point of polymer-modified and unmodified asphalt-binders with HMA rutting performance under the Accelerated Loading Facility (ALF). They reported that the conventional asphalt-binder parameters were unable to adequately correlate with HMA field rutting performance. Bahia and Anderson [18] compared a conventional parameter (i.e. viscosity) and a new asphalt-binder parameter (i.e., G*/ Sin δ) (1995). They explained that one of the main problems with conventional tests is their inability to measure parameters at the application temperatures and distinguish the viscoelastic nature of asphalt-binders. Bahia and Anderson [18] argued that a measure of viscosity alone cannot be enough to screen and select asphalt-binders with better rutting resistance.

Zhang et al. [15] compared two high-temperature rheological parameters of asphalt-binders (i.e., J_{nr} and G*/ Sin δ) and two HMA rutting related performance tests (HWTT and RLPD tests) for characterizing the asphalt-binder high-temperature properties relative to HMA rutting performance. For the limited asphalt-binders and HMA mixes evaluated, the J_{nr} parameter exhibited a relatively fair correlation (R^2>40%) with the HWTT and RLPD tests.

Limited studies have attempted to correlate asphalt-binder properties with field HMA rutting performance. A study by Chen and Tsai (1999) investigated the effects of asphalt-binder properties on the rutting performance of eight different pavement sections [35]. In their study, G*/ Sin (δ) was used to characterize the asphalt-binder rheological properties and correlated with field HMA rutting data. A fair correlation (R^2 = 44%) was found between G*/ Sin (δ) and field HMA rut depth. Another study by Anderson and Bukoski [36] correlated the J_{nr} with the HMA rutting measurements under the ALF and in-service pavement sections in the State of Mississippi, USA. Linear regression models were successfully used that presented coefficients of determination (R^2) exceeding 70% [36], thus, demonstrating the ability of the J_{nr} to improve the original G*/ Sin δ parameter.

Overall, the literature review indicated that most of the previous studies focused on correlating asphalt-binder properties with the rutting performance of laboratory compacted HMA samples. Limited studies have attempted to correlate the asphalt-binder properties with field rutting performance. Therefore, more laboratory testing and correlation and validation of field performance are still warranted to complement the results and findings presented in the literature. In particular, a three-line laboratory-field study, directly relating the MSCR (asphalt-binders) to HWTT (HMA mixes) to actual field HMA rutting performance, was deemed necessary. Thus, such an opportunity was offered in this study to develop and validate the relationships between the asphalt-binder MSCR test results and HMA rutting performance, both in the laboratory (HWTT) and field.

STUDY OBJECTIVES

In general, the main goal of this laboratory-field study was to assess the effects of asphalt-binder high-temperature properties on the HMA mix rutting resistance and HMA field rutting performance of in-service Texas highways sections. The specific objectives were as follows:

a) To characterize, quantify, and rank the rheological properties at high temperatures from the MSCR test of various widely used Texas asphalt-binders.
b) To characterize, quantify, and rank the laboratory rutting resistance of the corresponding Texas HMA mixes based on the HWTT test.

c) To quantify and rank the field rutting performance of the corresponding HMA mixes based on the evaluation of in-service Texas highway sections.

d) To correlate the laboratory test data, namely MSCR and HWTT, to field HMA rutting performance and establish statistical correlative models for evaluating the field HMA rutting performance.

e) To ascertain which asphalt-binder MSCR parameter provided the best statistical correlation with the HWTT test results and field HMA rutting performance data.

The paper is structured as follows: the test methods for asphalt-binders and HMA mixes are presented in the next section. The laboratory test results and field performance are then analyzed, including the laboratory-field performance correlations. Discussions of the analysis results are then introduced, and summaries and conclusions are presented in the last sections.

EXPERIMENTAL DESIGN PLAN

The Texas Pavement Database – The DSS

As previously mentioned in the introduction, the Texas DSS was the primary data source for asphalt-binders, HMA mixes, and field performance used in this study [37]. The DSS was developed, managed, and maintained in the user-friendly and readily accessible Microsoft Access® platform with 115 in-service asphalt pavement test sections and comprehensive laboratory test results and field performance data. These data include pavement design and construction, material properties of different pavement layers, including those measured in the laboratory and field, traffic load spectrum, climate history, existing pavement distresses for asphalt overlays, and field performance that has been evaluated bi-annually since 2010. Fig. 1 shows the DSS main screen interface and field site locations.

The extensive layer material properties in the Texas DSS, among many others, include the asphalt-binder rheological properties from the MSCR test and HMA rutting from the HWTT, which are the subject of this paper.

MSCR Test

The MSCR test is a creep and recovery test based on ASTM D7405 standard procedure [29]. This test method is typically conducted on Rolling Thin-Film Oven Test (RTFO) aged asphalt-binder samples of 25 mm in diameter and 1 mm in thickness at specified temperatures, which is controlled using a water bath in the DSR machine setup. The asphalt-binder samples were loaded at constant stress for 1 sec, then allowed to recover for 9 sec. Twenty creep and recovery cycles were run at 0.10 kPa creep stress level followed by 10 creep and recovery cycles at 3.20 kPa creep stress level [28,29]. The first 10 cycles at 0.10 kPa creep stress level were for conditioning the sample, allowing no rest period between the cycles [28,29]. A schematic representation of the MSCR test loading sequence is shown in Fig. 2.

The MSCR test measures and generates various parameters that are indicative of various high-temperature performance characteristics of the asphalt-binder [38], presented in Table 1 and Fig. 3. The primary MSCR output parameter is the non-recoverable creep compliance ($J_{nr_{3.2}}$), which has shown promising potential to evaluate the asphalt-binder rutting potential and predict HMA rutting performance [15,16,21,22,37,38].

HWTT Test

Based on the Tex-242-F specification, the following HWTT test setup was followed: 72 kg (158 lb.) vertical load at a wheel speed of 52 passes/min to 20000 passes at 50 ±1 °C (122°F) in a water bath [39]. These conditions were used for generating all the HWTT curves. Fig. 4 shows the HWTT device, the specimen dimension (150 mm diameter and 62.5 mm and ± 2 mm height) and the testing configuration.

The test termination criteria are based on either reaching a rut depth of 12.5 mm or the maximum number of load passes, whichever comes first. Additionally, the maximum number of load passes is different for different asphalt-binder PG, the maximum number of load passes for PG 64-XX, PG 70-XX and PG 76-XX are 10000, 15000 and 20000, respectively [39]. As presented in Table 2, some alternative HMA rutting parameters were proposed to supplement the criteria above [5,6,40-42]. In the next section, the standard and alternative parameters were comparatively evaluated.

Additionally, the creep slopes (mm/number of passes) of the rutting accumulative curves in Fig. 5 were also determined and evaluated, as they are directly related to the HMA rutting performance [43-45]. For the purposes of simplicity, linear slopes of the creep phase were used to represent the rate of rutting accumulation.

Asphalt-binders and HMA Mixes

In this study, the asphalt-binders comprised of PG 64-22. Two types of Texas HMA mixes were used, namely Type C and Type D, respectively. The respective asphalt-binders and HMA volumetric properties are listed in Table 3 along with the in-service highways constructed using the corresponding HMA mixes. As shown in Table 3, a commonly used Texas asphalt-binder grade PG 64-22 from different sources/suppliers was evaluated. The aggregate gradations comprised two coarse-graded Type C mixes (18.75 mm NMAS) with one fine-graded Type D mix (12.50 mm NMAS). The asphalt-binder contents were from 4.6 to 5.1%. The aggregates included limestone, dolomite, quartzite with RAP and RAS. The material composition difference could be used to represent the effects of material types, sources, volumetric properties, and mix types.

As per DSS protocol, the MSCR tests with three replicates were based on asphalt-binder extractions from plant-produced mixes that were hauled directly from the job construction sites. Due to oxidative aging that occurs during production and transportation to the job construction sites, the asphalt-binders were taken as RTFO aged. A chemical extraction method was used for the extraction of the asphalt-binders from plant-mixes with no extra laboratory aging. Similarly, all the HMA samples for the HWTT testing were molded and fabricated from plant-produced mixes to a target density of 93±1% using the Superpave gyratory compactor (SGC) [39]. In line with the DSS requirements, a minimum of three replicates were prepared and tested.

Approximately 1.5 hours of re-heating was required to break and loosen the HMA mixes prior to compaction. After compaction in the SGC, the HMA specimens were saw-cut to the required HWTT sample dimensions in Tex-242-F. The densities of HMA samples were also determined, and those which didn’t meet the target density were discarded. To reduce undesired aging, all the HWTT specimens were tested within five days after fabrication. Coefficient of variation (CoV) less than 30% was used as a threshold measure of variability in the data [40].

In-Service Test Sections

Five overlay test sections paved using the same asphalt-binders and mixes were selected in this study. As evident in Table 4, the test sections are in different climate zones with maximum summer temperatures above 50°C, more than 500 daily ESALs in the outside lane, and a service life over 5 years.

LABORATORY TEST RESULTS AND ANALYSIS

The MSCR Test Results

The asphalt-binder R and J_{nr} parameters in Table 1 were determined using the MSCR raw data. The corresponding average MSCR test results at 58°C and 64°C are shown in Tables 5 and 6, respectively. These averages were calculated using the results of three replicate samples.

From Tables 5 and 6, the R and J_{nr} parameters, as theoretically expected, exhibited dependency on temperature and stress level, namely while the R value decreased with increasing temperature and/or stress level, the J_{nr} value increased. In theory, asphalt-binders with larger J_{nr} values were more susceptible to rutting, since this means that the material had a large residual strain per each load cycle of applied stress. As noted in Tables 5 and 6, US 59 (TxDOT-TTI_00001 and TxDOT-TTI_00064, located in the highest temperature climate zone, see Table 4) exhibited the largest J_{nr} value at each temperature and stress level. On the other hand, US 83 (TxDOT-TTI_00041 and TxDOT-TTI_00081) showed the lowest J_{nr} value indicating higher rutting resistance.

From Tables 5 and 6, the ranking of the rutting resistance based on the $J_{nr_{0.1}}$ and $J_{nr_{3.2}}$ magnitude at both temperatures is as follows: US 83 (PG 64-22$_{c1}$) > SH 21 (PG 64-22$_{c2}$) > US 59 (PG 64-22$_{d}$). That is US 83 (PG 64-22$_{c1}$) exhibited the least permanent deformation (lowest J_{nr} values), while US 59 (PG 64-22$_{d}$) accumulated the most permanent deformation (highest J_{nr} values). A similar ranking is noted when considering the percent recovery (i.e., the higher the *R* value, the better), with US 83 (PG 64-22$_{c1}$) exhibiting the best elastic recovery properties (highest *R* values) while US 59 (PG 64-22$_{d}$) was the poorest (lowest *R* values). Since all the asphalt-binders are of the same grade/type, i.e., PG 64-22, the differences in the MSCR test results, ranking, and performance of the asphalt-binders could mainly be attributed to the differences in the source/suppliers and the potential additive effects (e.g., lime and RAP/RAS), particularly that the MSCR tests were conducted on the asphalt-binders extracted from the plant-produced HMA mixes. Therefore, it can be theoretically inferred that the source/supplier of an asphalt-binder affected its high-temperature properties.

The $J_{nr_{diff}}$ parameter, however, which is a measure of the asphalt-binder stress-sensitivity, must satisfy the AASHTO-ASTM $J_{nr_{diff}} \leq 75\%$ requirement [28,29]. As evident from Tables 5 and 6, the $J_{nr_{diff}}$ values for all the tested asphalt-binders were below that threshold. On the other hand, the reviewed literature did not report any insights on the relationship between *R* and HMA rutting resistance. Instead, the *R* parameter has been reported to show promising potential as an indicative measure of the elastic response of asphalt-binders [28,29,47], which allows to identify and quantify the asphalt-binder modification with elastomeric polymers (Fig. 6).

A standard MSCR curve, relating the $R_{3.2}$ and $J_{nr_{3.2}}$ was used to examine whether the tested asphalt-binders exceeded the $R_{3.2_{min}}$[47] in Fig. 6, $R_{3.2_{min}}$ is the minimum required values of $R_{3.2}$ to indicate significant elastic behavior and $J_{nr_{3.2}}$ is the measured value of non-recoverable creep compliance at 3.2 kPa.

Data points that are plotted on or above the MSCR curve are considered to have a significant elastic response, indicating that the asphalt-binder has been modified with elastomeric polymers [47]. From Fig. 6, none of the asphalt-binders evaluated in this study (i.e., all comprising of PG 64-22) had a high elastic response, i.e., high elasticity. All the *R* values are less than 55% (i.e.,$R_{0.1}, R_{3.2} \leq$ 55% both at 58 and 64°C), thus, indicating poor elasticity and no presence of polymer modification. Thus, true to the designated high-temperature grade and considering the $R_{3.2_{min}}$ criteria [47], the PG 64-22 asphalt-binders, indeed, are all unmodified asphalt-binders without any indication of polymer modifiers.

The HWTT Test Results

The HWTT accumulative rutting curves for the Types C_1, C_2 and D mixes are plotted in Fig. 7. The ranking of HMA mix superiority based on the measured *RD* at 10000 N_d is as follows: Type D (3.40 mm) > Type C_1 (4.05 mm) > Type C_2 (5.36 mm), all of them significantly lower than the terminal threshold (i.e., $RD \leq 12.5$ mm).

An interesting point is that the fine-graded Type D mix with prime quartzite aggregates, 10.2% coarse RAP, and 9.9% fine RAP showed better performance than the coarse-graded Type C mixes with only fine RAP/RAS additives at both 10000 and 20000 N_d. In fact, the worst performer at N_d = 20000 was the Type C_1 mix with the *RD* of 9.40 mm. Furthermore, the Type C_1 rutting curve exhibited a different shape from the Type C_2 and D mixes, with relatively rapid rutting occurring after N_d = 8000, indicating that moisture damage might have occurred. As evident in Table 3, while Type C_2 had 1% lime, no anti-stripping agent was included in the Type C_1 despite having moderate quality limestone aggregates.

Numerous other HWTT rutting parameters in Table 2 were also calculated at N_d =10000 [37]. All the HMA mixes evaluated comprised of PG 64-22 asphalt-binder whose *RD* failure criteria according to the Tex-242-F specification is defined at N_d =10000 HWTT load passes.

According to Table 7, all the HMA mixes meet the Rut_Δ criteria (i.e., $Rut_\Delta \leq 8.0$) proposed in Table 2, the smaller values of Rut_Δ and/or Δ_A in Column 5, the greater rutting resistance. Therefore, the ranking of rutting resistance in terms of these rutting parameters are as follows: Type D > Type C_1 > Type C_2, which are the same as that for the *eRL*, *RRI*, *RR*, and *Slope* parameter. In particular, the highest remaining life for the Type D mix was identified using the *eRL*.

The test results in Fig. 7 and Table 7 are consistent with the HMA mix-design characteristics in Table 3. The moderately quality limestone/dolomite aggregates were used in coarse-graded Type C (Types C_1 and C_2). Particularly, the Type C_2 mix had about 1% lime to mitigate against possible moisture damage, while the Type C_1 mix had no anti-stripping agent. The Type D mix used quartzite aggregates that are generally durable and moisture resistant.

Additionally, about 10.2% coarse fractionated RAP was used in the Type D mix whereas only fine RAP was used in the Type C_1 and C_2 mixes. It is expected that the 10.2% coarse fractionated RAP contributed to better rutting resistance. Theoretically, HMA mixes with coarser aggregates are expected to perform better against rutting. However, in this particular study, Type D mix, with a fine-graded gradation, outperformed the coarse-graded, Type C_1 and C_2 mixes. This could be explained by the fact that the Type D mix included 10.2% of coarse RAP, while all the RAP and RAS used in Type C_1 and C_2 mixes are fine-graded. Furthermore, some other factors, such as differences of aging levels, material types/sources, asphalt-binder contents and gradations of the RAP/RAS could alter the true PG of the asphalt-binder and the rutting resistance of the HMA mix. However, detailed chemistry evaluation of the asphalt-binder, RAP/RAS, and lime was outside the scope of this study.

Laboratory Test Comparisons and Material Rankings

In consideration of the MSCR and HWTT test results in Tables 5, 6 and 7, the overall ranking in order of superiority of the asphalt-binder and HMA mixes in terms of rutting resistance is summarized in Table 8. The ranking of rutting resistance of the asphalt-binders based on the $J_{nr_{0.1}}$ and $J_{nr_{3.2}}$ parameters at 58 and 64°C, is as follows: PG 64-22_{c1}> PG 64-22_{c2} > PG 64-22_{d}. Although the PG grade of all three asphalt-binders is the same, the difference in performance could be attributed to variations in the material sources/supplier and the effects of the additives, among other factors.

In the case of the HWTT test results, the rutting parameters computed, namely *RD, Slope*, Δ_A, Rut_Δ, *eRL*, *RR*, and *RRI*, exhibited the same ranking based on the HMA rutting resistance as follows: Type D > Type C_1 > Type C_2. As previously discussed, the Type D mix comprised high-quality quartzite aggregates and about 10.2% coarse fractionated RAP, whereas moderate-quality limestone/dolomite aggregates and only fine RAP were used in the Type C_1 and C_2 mixes.

Overall, the test results in Table 8 show that, in fact, HMA rutting is a complex distress mechanism to evaluate that is interactively affected by many factors, including asphalt-binder and aggregate properties. Whereas, the MSCR only takes into consideration asphalt-binder characteristics, the HWTT takes into consideration the interaction of many variables (asphalt-binder, aggregates, RAP/RAS, AVs, etc.). Therefore, this partly explains the differences in the rank order of material (asphalt-binders and HMA mixes) superiority between MSCR and HWTT.

Laboratory Test Data Quality, Consistency, and Statistical Variability

The acceptability of the MSCR test results in Table 1 was analyzed following the ASTM repeatability and reproducibility thresholds of ASTM D 7405 [20]. The laboratory MSCR test results in Tables 5 and 6 represents an average of the three sample replicates. PG 64-22_{c1},PG 64-22_{c2}, and PG 64-22_{d}, for example, have CoV values of $R_{0.1}$ @ $64°C$=5.99%, 3.90%, 0.01%, $R_{3.2}$ @ $64°C$=4.60%, 4.43%, 2.45%, $J_{nr_{0.1}}$ @ $64°C$ =0.65%, 4.58%, 4.11% and $J_{nr_{3.2}}$ @ $64°C$ =1.40%, 4.31%, 1.94%, respectively, that all meet the ASTM D 7405 limits (i.e., $R_{0.1} \leq$ 6.7%, $R_{3.2} \leq$ 8.5%, $J_{nr_{0.1}} \leq$ 38.3%, and $J_{nr_{3.2}} \leq$ 26.6%) [29]. Thus, the MSCR test data used in this study is of acceptable quality and lends statistical confidence in the findings and conclusions drawn thereof.

On the other hand, low variability (i.e., CoV ≤ 30%) is shown in the HWTT results in Table 7 with a minimum of three replicates. The Type D (fine-graded) mixes generally exhibited better consistency with lower variability than the Type C (coarse-graded) mixes. Overall average CoV values for Types D and C mixes are 2.1% (0.1% to 7.4%) and 8.9% (1.5% to 24.9%), respectively.

It is shown that the CoV values are below the specification limits, substantiating the repeatability, data consistency, and data quality of the MSCR and HWTT results. Note that this better repeatability and low variability in the test data, for both the MSCR and HWTT, were partly attributed to professionality and proper machine calibration. These aspects can be substantiated by the AVs data presented in Table 7 that satisfactorily falls within the 7±1% AVs target range. In fact, the AVs range in Table 7 is only 6.49% to 7.22% (versus the 6.0-8.0% allowable range), with the corresponding CoV ranging from 1.98% to 18.19%, which is less than the 30% threshold that was used as a measure of statistical variability in this study.

FIELD RUTTING PERFORMANCE AND DATA ANALYSIS

This section presents the field rutting performance and analysis of the five test sections in Table 4. The main output data of the field rut measurements is the total RD of the pavement structure. For field performance evaluation, TxDOT specifies four severity levels based on the total *RD*, as follows: (a) shallow (6.25 -12.25 mm), (b) deep (12.50 -24.75 mm), (c) severe (25.00 – 49.75 mm), and (d) failure (≥ 50 mm). Fig. 8 shows the rutting performance measured on the highway test sections for over six years period of service life, as extracted from the DSS. The field performance presents that all of the sections showed good early-life rutting resistance, since the total surface *RD* measured were less than 9.8 mm, which is classified as shallow rutting and below the 12.50 mm *RD* terminal criteria for deep rutting [5,33]. Additionally, these field results further validated the HWTT screening criteria.

However, to effectively compare and correlate the MSCR and HWTT laboratory results with field performance, only the respective HMA surface layer contribution should be considered. Percent rutting of the corresponding HMA surface layers was estimated based on Faruk et al.'s method of mechanistic-empirical (M-E) modeling of the pavement structures using the AASHTOWare Pavement ME Design [48]. Each pavement was modelled including the pavement structure, traffic load spectrum, layer material properties, and climatic conditions in Table 4.

The computed percentage contributions of HMA surface layer were as follows: SH21[EB]_TypeC_2 = 18.00%, US59[SB]_TypeD= 13.06%, US59[NB]_TypeD= 13.61%, US83[EB]_TypeC_1 = 8.33%, and US83[WB]_TypeC_1= 11.28%. The determined percentage rutting contributions were then used to approximate the HMA surface layer *RD* from the total *RD* measured in Fig. 8. Details of this method can be found in the literature [48].

On the other hand, to account for the effect of traffic level, the field rutting was normalized as a function of cumulative equivalent single axle loads (ESALs). The cumulative ESALs (Million) were estimated using Eq. (1) and the traffic data shown in Table 4 [49].

$$W_{18(n)} = 0.5n(365 * W_{18(d)})(1 + (1 + G_r)^n) \quad (1)$$

Where $W_{18(n)}$= cumulative n-year 18-kip ESALs; n= analysis period in years; $W_{18(d)}$=daily 18-kip ESALS (DESALs); and G_r= traffic growth rate (decimal). The HMA field rutting performance of the selected in-service highway sections are illustrated in Figs. 9 and 10.

The HMA layer rutting performance versus pavement age is shown in Fig. 9. The field performance shows that all HMA layer RDs are below 1.00 mm. SH 21[EB]_TypeC_2 (i.e., TxDOT-TTI_00042) recorded the maximum HMA layer rutting, which was expected due to the high pavement temperature of 52.8°C (at 1-inch depth) and high traffic loading of 1450 DESALs. Using 6.23-year service life as the benchmark, the US59 [NB]_TypeD (i.e., TxDOT-TTI_00064) showed the best rutting resistance.

The rutting accumulation/propensity of the HMA layers was assessed using the *Slope A* (mm/years) of the rutting response-curves using linear regression. Overall, the ranking for HMA rutting resistance based on *Slope A* would be as follows: US83[WB]_TypeC_1 (0.070 mm/year) >US59[NB]_TypeD(0.074mm/year)>US59[SB]_TypeD(0.092mm/year)>US83[EB]_TypeC_1 (0.115mm/year) > SH 21[EB]_TypeC_2 (0.137 mm/year).

Fig. 10 shows the HMA layer rutting performance plotted as a function of traffic load expressed in terms of ESALs. All the field HMA layers exhibited superior rutting performance with *RD* values much less than 1.00 mm [31]. Using 2.68 million ESALs (MESALs) as the reference point, US83[WB]_TypeC_1 and US59[SB]_TypeD (i.e., TxDOT-TTI_00081 and TxDOT-TTI_00001, respectively) would be in the upper rank of superior rutting resistance performance. SH 21[EB]_TypeC_2 followed by US83[EB]_TypeC_1 (i.e., TxDOT-TTI_00042 and TxDOT-TTI_00041, respectively) would be in the lower rank.

Like *Slope A,* the RD accumulation rate for the HMA layers was assessed using *Slope B* (mm/MESALs) with linear regressions. The ranking for *slope B* would be as follows: US59[SB]_TypeD (0.096mm/MESALs) > US83[WB]_TypeC_1 (0.110 mm/MESALs) > US83[EB]_TypeC_1 (0.155mm/MESALs) > US59[NB]_TypeD (0.195 mm/MESALs) > SH

21[EB]_TypeC_2 (0.247 mm/MESALs). Coincidently, the results are consistent with the HWTT test results and laboratory predictions shown previously in Fig. 7 (at N_d = 10000) and Table 8, respectively.

LABORATORY AND FIELD CORRELATIONS

Correlation strength of the MSCR test results to HWTT and field HMA rutting performance was evaluated in terms of the coefficient of determination (R^2) based on the Table 9 proposed criteria. The correlation rating has five levels, with *A* representing a very good correlation strength with $R^2 \geq 60$ %, while *E* represents a very poor correlation strength with $R^2 < 10\%$. These proposed criteria were arbitrarily selected with the consideration that good statistical correlations with higher R^2 values between laboratory and field performance data are often not so common.

Firstly, the MSCR parameters were correlated using linear, power, exponential and logarithmic fit models with the aim of selecting the best regression model. The corresponding results at two different temperatures are shown in Tables 10 and 11.

From Table 11, $R_{0.1}$, $R_{3.2}$, and R_{diff} showed very good correlation strength with $J_{nr_{0.1}}$, $J_{nr_{3.2}}$, and $J_{nr_{diff}}$ at 58°C and 64°C, with most of the R^2 values above 60% for all the four regression equations. Note that R^2 values were higher for correlations at 64°C, particularly with the linear and/or exponential regression models. The exponential model exhibited the best regression with an R^2 =100.00% in the correlation between $R_{0.1}$ and $J_{nr_{3.2}}$ both at 64°C. The relationship between $R_{3.2}$ and $J_{nr_{3.2}}$ has been previously evaluated with most researchers suggesting that the best regression is obtained with a power model [36,47]. In this study, the aforementioned correlation showed R^2 values of 98.40% and 95.49% for 58°C and 64°C, respectively, which concurs with the literature reports [36,47,50].

Overall, these generally good correlations were expected since both parameters (R and J_{nr}), were determined from the same asphalt-binders and MSCR test. Looking at Tables 10 and 11 for the PG 64-22 asphalt-binder evaluated in this study, the overall best fit-model appears to be the exponential function.

Asphalt-Binder MSCR versus HMA Lab Rutting (HWTT)

The correlation of the MSCR parameters at 58°C and 64°C with the HWTT results at N_d=10000 was evaluated with the aim of formulating models to predict the HMA rutting potential. The corresponding results are shown in Tables 12 and 13. Note that both the conventional and alternative HWTT parameters at N_d=10000 were used and analyzed for correlations with the MSCR test data.

Overall, the rank order of superiority in terms of correlation of the MSCR percent recovery parameters at 58°C to HWTT laboratory results at N_d=10000 based on the R^2 magnitude is: $R_{diff} > R_{0.1} > R_{3.2}$, with power and/or logarithmic models as the best regression. Besides, in terms of correlation of MSCR for the non-recoverable creep compliance parameters, the overall ranking based on R^2 magnitude is: $J_{nr_{diff}} > J_{nr_{0.1}} > J_{nr_{3.2}}$, with linear and/or exponential models as the best regression.

Looking at Table 13, the correlations at 64°C were relatively poor with R^2 values lower than those at 58°C. For example, $R_{0.1}$ and $R_{3.2}$ passed from a fair/good correlation to a poor/very poor correlation with *RD, eRL, RR, and Slope* with R^2 values below 20%. A similar trend was observed for the R_{diff}, $J_{nr_{0.1}}$, and $J_{nr_{3.2}}$ parameters. However, $J_{nr_{diff}}$ at 64°C had a different behavior exhibiting superiority even over the correlations shown with $J_{nr_{diff}}$ at 58°C with all the HWTT parameters, particularly with power and/or logarithmic models as the best regression having R^2 values above 80% (e.g., R^2 = 99.87% for $J_{nr_{diff}}$ at 64°C versus *RD* and/or *Slope* in a power model).

Note that the correlations of MSCR at 58°C to HWTT at N_d= 10000 had higher R^2 values than those of the MSCR at 64°C, which may be due to the fact that the HWTT was tested at a lower temperature of 50°C, which is closer to 58°C than 64°C. The test temperatures of these two tests (i.e., MSCR and HWTT) do not match and, it appears that the R^2 values decreased when the temperature difference between them increased. Thus, the correlations of MSCR at 58°C to HWTT at N_d=10000 were the best for the materials evaluated in this study. In addition, considering the results in Table 12 and the fact that there are no previous studies reviewed in the literature on the relationship between the percent recovery parameters and HMA rutting performance, $R_{0.1}$, $R_{3.2}$ and R_{diff}, all at 58°C, should be used with caution to predict laboratory rutting resistance of HMA mixes.

Lastly, the $J_{nr_{0.1}}$, $J_{nr_{3.2}}$, and $J_{nr_{diff}}$ parameters at 58°C, as theoretically expected, have superior correlations with the HWTT results at N_d=10000 than the *R* parameters. Thus, $J_{nr_{0.1}}$, $J_{nr_{3.2}}$ and $J_{nr_{diff}}$ parameters, all at 58°C had reasonably acceptable predictive potential to grade asphalt-binders in terms of predicting HMA rutting performance in the laboratory.

However, $J_{nr_{3.2}}$ was proposed and recommended by the FHWA as the parameter for asphalt-binder grading [15]. For the materials evaluated and test conditions considered in this study, it is shown that the $J_{nr_{diff}}$ at 58°C and 64°C were the best high-temperature parameter of asphalt-binders to predict and correlate to the HMA laboratory rutting performance, and therefore, can be used to supplement the $J_{nr_{3.2}}$ FHWA recommendation.

Asphalt-Binder MSCR versus HMA Field Rutting Performance

The correlation of the MSCR parameters at 58°C and 64°C with the field HMA rutting performance was evaluated with the main goal of evaluating the HMA mixes rutting potential in the field based on the rheological properties. The corresponding R^2 values for the four different regression models used are listed in Tables 14 and 15. The field HMA rutting parameters evaluated were as follows: (a) *RD* at 6.23 years of service life, (b) *RD* at 2.68 MESALs of traffic loading, (c) *Slope A* (mm/year), and (d) *Slope B* (mm/MESALs).

Based on Table 9, for the four regression models used, all the MSCR parameters at 58°C and 64°C, with the exception of $J_{nr_{diff}}$, showed very poor to fair correlations (i.e., $R^2 < 40$ %). This indicates their undesirable low prediction accuracy to correlate with the HMA field rutting performance. On the contrary, $J_{nr_{diff}}$ at both 58°C and 64°C exhibited a superior correlation strength. For instance, $J_{nr_{diff}}$ *(%)* at 58°C showed a good to very good correlation with all the rutting parameters, particularly with linear and/or exponential models as the best regression (e.g., R^2=71.62% for $J_{nr_{diff}}$ *(%)* at *58*°C versus *RD 2.68 MESALS* in linear model). As for $J_{nr_{diff}}$ *(%)* at 64°C, it showed the best and strongest correlation with all the rutting parameters, especially for the *RD 6.23 years* parameter that had R^2 values as high as 76.01% and 79.48% with power and logarithmic regression models, respectively.

HMA (HWTT) versus HMA Field Rutting Performance

Based on a previous study evaluated the correlation of HWTT to HMA field rutting performance [51], most of the HWTT rutting parameters generally present very good correlation with the HMA field rutting performance. The results, in fact, suggested that all the HMA HWTT rutting parameters at N_d= 10000, except for *SF*, are promising performance predictors of HMA field rutting, particularly, Rut_{Δ} and Δ_{A} parameters with R^2 averaging 69.92%.

SYNTHESIS AND DISCUSSION OF THE RESULTS

From the MSCR test results, the percent recovery (R) and non-recoverable creep compliance (J_{nr}) parameters at 58°C and 64°C, were correlated with the conventional and alternative HWTT parameters at N_d =10000. Thereafter, both the laboratory MSCR and HWTT test data were correlated to the HMA field rutting performance of five selected sections from the DSS. A graphical comparison of these results is presented in Fig. 11.

Fig. 11 shows a graphical contrast of some selected MSCR, HWTT, and HMA field rutting parameters evaluated in this study. Fig. 11 (a) indicates three graphs that have a similar trend, which represents good to very good correlation strength between $J_{nr_{diff}}$ at 58°C versus the HWTT and HMA field rutting performance. Theoretically, this means that $J_{nr_{diff}}$ at 58°C could reasonably predict the HMA HWTT and field rutting resistance, respectively. By contrast, Fig. 11 (b) exemplifies an opposite response trend, evidencing the lower prediction accuracy of $R_{0.1}$ at 58°C to correlate and/or estimate the HMA rutting resistance in the laboratory and field. Therefore, the $R_{0.1}$, $R_{3.2}$, and R_{diff} parameters, should be used with caution when predicting the HMA laboratory and field rutting resistance potential.

For the HMA mixes in the HWTT, the differences in the aggregate gradations had a key effect on the mix rutting performance. On the other hand, the materials (asphalt-binder and aggregate), the pavement structure, traffic level, and temperature all interactively contributed to the observed differences in the HMA field rutting performance. However, detailed aggregate evaluation was outside the scope of this study, with recommendations for inclusion in future follow-up studies. On the other hand, the materials (asphalt-binder and aggregate), the pavement structure, traffic level, and temperature all interactively contributed to the observed differences in the HMA field rutting performance. Nonetheless, informative results were provided in this study in terms of the validations and correlations of the high-temperature rheological properties from the MSCR test to the mixes properties from the HWTT and field HMA rutting performance.

CONCLUSIONS AND RECOMMENDATIONS

In this study, the asphalt-binder high-temperature rheological properties were correlated to the HMA rutting performance measured in the laboratory and field, respectively. The main objective of the study was to assess the capability of the asphalt-binder high-temperature properties including J_{nr} and R parameters to correlate and predict the HMA rutting resistance in the laboratory and field. Based on the results and findings in the paper, the following conclusions and recommendations were drawn.

- Even though the asphalt-binder percent recovery properties (i.e., $R_{0.1}$ and $R_{3.2}$) have no reported literature of good correlation with HMA mix rutting performance, some good laboratory correlations with the HWTT rutting data were found in this study, particularly the R_{diff} parameter, i.e., $40 \leq R^2 < 60\%$. However, the correlations were poor for the field rutting performance data, with the R^2 values less than 40%. In general, any HMA rutting predictions based on the asphalt-binder percent recovery properties (i.e., R parameters) should be analyzed cautiously and interpreted subjectively. The R parameters are better suited for characterizing and quantifying the modifier presence in the asphalt-binders.
- For the asphalt-binder non-recoverable creep compliance parameters, the $J_{nr_{diff}}$ from the MSCR test, generally exhibited good to strong statistical correlations, with R^2 values as high as 98.9% and 79.5% for laboratory and field correlations, respectively. Thus, the $J_{nr_{diff}}$ parameter is recommended for predicting the HMA rutting resistance in terms of effects of the asphalt-binder, both in the laboratory and field.
- Based on the data evaluated in this study, the results and findings indicated that the linear and logarithmic regressions were the best fit-functions correlate the asphalt-binder high-temperature properties (i.e., $J_{nr_{diff}}$ at 58°C and 64°C, respectively) to HMA rutting in the laboratory and field.
- While only PG 64-22 asphalt-binder was used, but from three different sources was used, some differences in terms of the high-temperature rheological properties and performance were observed, which were largely attributed to the effects of

source/supplier and/or the possible additives, particularly considering that the MSCR tests were conducted on the asphalt-binders extracted from the plant-produced HMA mixes.

- As expected, the Type D mix comprising of highly quality quartzite aggregates and coarse-fractionated RAP, out-performed the mixes with limestone/dolomite aggregates and fine-fractionated RAP. Similarly, the field rutting performance of the HMA mixes was consistent with the HWTT laboratory test results and predictions. Evidently, the findings indicate that using coarse-fractionated RAP is more beneficial over fine-fractionated RAP in terms of improving the rutting resistance potential for the HMA.

Generally, the findings of this paper demonstrated that the asphalt-binder high-temperature properties could be used to predict the HMA rutting resistance in the laboratory and field with acceptable statistical reliability, particularly the $J_{nr_{diff}}$ parameter. Due to the limited data, the results in this study might not be exhaustive Therefore, in future studies, more data including different types of asphalt-binder, HMA mixes, and field performance along with varying the MSCR test loading/recovery times is recommended to supplement and validate the findings reported in this paper. When considering the field performance, field conditions such as traffic levels, climatic variations, and pavement structures are also important. Additionally, other advanced statistical models along with 3-dimensional analysis (i.e., asphalt-binder [x], HMA [y], and field [z]) need to be explored to assess if better correlations with improved prediction accuracy could be yielded.

DATA AVAILABILITY STATEMENT

All data, models, and code generated or used during the study appear in the submitted article.

ACKNOWLEDGEMENTS AND DISCLAIMER

The authors thank all those who assisted in this study including laboratory testing, field work, data collection, data compilation, analysis, and documentation of this paper. The authors also gratefully acknowledge the Texas flexible pavements and overlays database (DSS) that valuably served as the primary data source for the work presented in this paper.

The contents of this paper reflect the views of the authors who are solely responsible for the facts and accuracy of the data presented herein and do not necessarily reflect the official views or policies of any agency or institute. This paper does not constitute a standard, specification, nor is it intended for design, construction, bidding, contracting, tendering, certification, or permit purposes. Trade names were used solely for information purposes and not for product endorsement, advertisement, promotions, or certification.

REFERENCES

1. National Asphalt Pavement Association, Engineering Overview, (n.d.). https://www.asphaltpavement.org/index.php?option=com_content&view=article&id=14&Itemid=33 (accessed July 13, 2019).
2. F.L. Roberts, L.N. Mohammad, L.B. Wang, History of Hot Mix Asphalt Mixture Design in the United States, J. Mater. Civ. Eng. 14 (2002) 279–293. doi:10.1061/(asce)0899-1561(2002)14:4(279).
3. Lytton, R. L., Uzan, J., Fernando, E. G., Roque, R., Hiltunen, D., & Stoffels, S. M. (1993). Development and validation of performance prediction models and specifications for asphalt binders and paving mixes (Vol. 357). Washington, DC: Strategic Highway Research Program.
4. L.F. Walubita, A.N. Faruk, S.I. Lee, D. Nguyen, R. Hassan, S. Tom, HMA Shear Resistance, Permanent Deformation, and Rutting Tests for Texas Mixes: Final Year-2 Report, 2014. http://tti.tamu.edu/documents/0-6744-2.pdf.
5. L.F. Walubita, S.I. Lee, J. Zhang, A.N. Faruk, S. Nguyen, T. Scullion, HMA Shear Resistance , Permanent Deformation , and Rutting Test For Texas Mixes : Year-1 Report, 2014. http://tti.tamu.edu/documents/0-6744-1.pdf.
6. L.F. Walubita, T. Nyamuhokya, S.I. Lee, A. Prakoso, Implementation of the HMA Shear Test for Routine Mix-Design and Screening : Technical Report, 2019. http://tti.tamu.edu/documents/5-6744-01-R1.pdf.
7. X. Hu, L.F. Walubita, Influence of asphalt-binder source on CAM mix rutting and cracking performance: A laboratory case study, Int. J. Pavement Res. Technol. 8 (2015) 419–425. doi:10.6135/ijprt.org.tw/2015.8(6).419.

8. Federal Highway Administration, Pavement Distress Identification Manual, 2009.
9. J.S. Miller, W.Y. Bellinger, Distress Identification Manual for Long-Term Pavement Performance Program, 5th ed., 2014.
10. US ARMY CORPS OF ENGINEERS, Asphalt Surfaced Airfield Paver Distress Identification Manual, 2009.
11. US ARMY CORPS OF ENGINEERS, Paver Asphalt Distress Manual, 1997.
12. Cartegraph, Standard Pavement Distress Identification Manual, 2014.
13. A. Arshadi, Importance of asphalt binder properties on rut resistance of asphalt mixture, University of Wisconsin-Madison, 2013.
14. G. Zou, J. Xu, C. Wu, Evaluation of factors that affect rutting resistance of asphalt mixes by orthogonal experiment design, Int. J. Pavement Res. Technol. 10 (2017) 282–288. doi:10.1016/j.ijprt.2017.03.008.
15. J. Zhang, L.F. Walubita, A.N.M. Faruk, P. Karki, G.S. Simate, Use of the MSCR test to characterize the asphalt binder properties relative to HMA rutting performance - A laboratory study, Constr. Build. Mater. 94 (2015) 218–227. doi:10.1016/j.conbuildmat.2015.06.044.
16. J.A. D'Angelo, The relationship of the mscr test to rutting, Road Mater. Pavement Des. 10 (2009) 61–80. doi:10.1080/14680629.2009.9690236.
17. H.U. Bahia, D.I. Hanson, M. Zeng, H. Zhai, M.A. Khatri, R.. Anderson, Characterization of Modified Asphalt Binders in Superpave Mix Design, 2001.
18. H.U. Bahia, D.A. Anderson, Strategic Highway Research Program Binder Rheological Parameters: Background and Comparison with Conventional Properties, Transp. Res. Rec. 1488 (1995) 32–39.
19. D. Singh, A. V. Kataware, Comparison of different rheological parameters for rutting

susceptibility of SBS + WMA modified binders, Innov. Infrastruct. Solut. (2016) 1–10. doi:10.1007/s41062-016-0026-7.

20. M.D.I. Domingos, A.L. Faxina, Susceptibility of Asphalt Binders to Rutting: Literature Review, J. Mater. Civ. Eng. 28 (2016). doi:10.1061/(asce)mt.1943-5533.0001364.
21. S. Dreesen, J.P. Planche, V. Gardel, A new performance related test method for rutting prediction: MSCRT, in: A. Loizos, M.N.. Part, T. Scarpas, I.L. Al-Qadi (Eds.), Adv. Test. Characterisation Bitum. Manterials, 2009: pp. 971–980.
22. N. Tabatabaee, H.A. Tabatabaee, Multiple Stress Creep and Recovery and Time Sweep Fatigue Tests: Crumb Rubber Modified Binder and Mixture Performance, Transp. Res. Rec. 2180 (2010) 67–74. https://doi.org/10.3141/2180-08.
23. J.G. Speight, Chapter 10 - Asphalt Paving, in: J.G.B.T.-A.M.S. and T. Speight (Ed.), Butterworth-Heinemann, Boston, 2016: pp. 409–435. doi:https://doi.org/10.1016/B978-0-12-800273-5.00010-6.
24. M. Southern, 1 - A perspective of bituminous binder specifications, in: S.-C. Huang, H.B.T.-A. in A.M. Di Benedetto (Eds.), Woodhead Publ. Ser. Civ. Struct. Eng., Woodhead Publishing, Oxford, 2015: pp. 1–27. doi:https://doi.org/10.1016/B978-0-08-100269-8.00001-5.
25. J.G. Speight, Chapter 9 - Asphalt Technology, in: J.G.B.T.-A.M.S. and T. Speight (Ed.), Butterworth-Heinemann, Boston, 2016: pp. 361–408. doi:https://doi.org/10.1016/B978-0-12-800273-5.00009-X.
26. American Society for Testing and Materials, ASTM D7552:Standard Test Method for Determining the Complex Shear Modulus (G*) Of Bituminous Mixtures Using Dynamic Shear Rheometer, 2014. doi:10.1520/D7552-09R14.

27. A. Behnood, A. Shah, R.S. McDaniel, M. Beeson, J. Olek, High-Temperature Properties of Asphalt Binders: Comparison of Multiple Stress Creep Recovery and Performance Grading Systems, Transp. Res. Rec. J. Transp. Res. Board. 2574 (2016) 131–143. doi:10.3141/2574-15.

28. Federal Highway Administration - US Department of Transportation, Asphalt Binder PGTests,n.d.https://www.fhwa.dot.gov/pavement/materials/hmec/pubs/module_f/lab_manual_asphalt.pdf.

29. American Society for Testing and Materials, ASTM D7405: Standard test method for Multiple Stress Creep and Recovery (MSCR) of asphalt binder using a dynamic shear rheometer, 2015. doi:10.1520/D7405-15.2.

30. T.L.J. Wasage, J. Stastna, L. Zanzotto, Rheological analysis of multi-stress creep recovery (MSCR) test, Int. J. Pavement Eng. 12 (2011) 561–568. doi:10.1080/10298436.2011.573557.

31. E. Masad, C.-W. Huang, J. D'Angelo, D. Little, Characterization of asphalt binder resistance to permanent deformation based on nonlinear viscoelastic analysis of multiple stress creep recovery (MSCR) test, 2009.

32. F. Yin, E. Arambula, R. Lytton, A.E. Martin, L.G. Cucalon, Novel Method for Moisture Susceptibility and Rutting Evaluation Using Hamburg Wheel Tracking Test, Transp. Res. Rec. J. Transp. Res. Board. 2446 (2014) 1–7. doi:10.3141/2446-01.

33. Zhang, Y., Ling, M., Kaseer, F., Arambula, E., Lytton, R. L., & Martin, A. E. (2021). Prediction and evaluation of rutting and moisture susceptibility in rejuvenated asphalt mixtures. Journal of Cleaner Production, 129980.

34. D. Sybilski, Evaluation of validity of conventional test methods in case of polymer-

bitumens, Am Chem Soc Div Fuel Chem. 41 (1996) 1302–1306.

35. Chen. J.S and Tsai, C.J. 1999. How good are linear viscoelastic properties of asphalt binder to predict rutting and fatigue cracking?, Journal of Materials Engineering and Performance, Vol. 8 (4), pp. 443-449.
36. M. Anderson, J. Bukoski, Using the Multiple-Stress Creep Recovery (MSCR), in: North Cent. Asph. User Prod. Gr. Meet., 2012.
37. L.F. Walubita, S.I. Lee, A.N.M. Faruk, T. Scullion, S. Nazarian, I. Abdallah, Texas Flexible Pavements and Overlays : Year 5 Report — Complete Data Documentation, 2017. http://tti.tamu.edu/documents/0-6658-3.pdf.
38. H. Soenen, T. Blomberg, T. Pellinen, O.V. Laukkanen, The multiple stress creep-recovery test: A detailed analysis of repeatability and reproducibility, Road Mat
39. Texas Department of Transportation (TxDOT), TEX-242-F: Test procedure for Hamburg Wheel-Tracking Test, 2014. https://ftp.dot.state.tx.us/pub/txdot-info/cst/TMS/200-F_series/pdfs/bit242.pdf.
40. L.F. Walubita, L. Fuentes, S.I. Lee, I. Dawd, E. Mahmoud, Comparative evaluation of five HMA rutting-related laboratory test methods relative to field performance data: DM, FN, RLPD, SPST, and HWTT, Constr. Build. Mater. 215 (2019) 737–753. doi:10.1016/j.conbuildmat.2019.04.250.
41. B.W. Tsai, E. Coleri, J.T. Harvey, C.L. Monismith, Evaluation of AASHTO T 324 Hamburg-Wheel Track Device test, Constr. Build. Mater. 114 (2016) 248–260. doi:10.1016/j.conbuildmat.2016.03.171.
42. H. Wen, S. Wu, L.N. Mohammad, W. Zhang, S. Shen, A. Faheem, Long-Term Field Rutting and Moisture Susceptibility Performance of Warm-Mix Asphalt Pavement, Transp. Res. Rec. J. Transp. Res. Board. 2575 (2016) 103–112. doi:10.3141/2575-

11.

43. P.S. Kandhal, J. L Allen Cooley, NCHRP Report 508-Accelerated Laboratory Rutting Tests: Evaluation of the Asphalt Pavement Analyzer, Washington,D.C., 2003. http://onlinepubs.trb.org/onlinepubs/nchrp/nchrp_rpt_508.pdf.
44. S. Schram, R.C. Williams, A. Buss, Reporting Results from the Hamburg Wheel Tracking Device, Transp. Res. Rec. J. Transp. Res. Board. 2446 (2014) 89–98. doi:10.3141/2446-10.
45. Illinois Department of Transportation (IDOT), Manual of Modified Test Procedures, 2019. https://www.illinoistollway.com/documents/20184/760479/01-Tollway+Manual+of+Test+Procedures_Final-03142019.pdf/7ee864b6-9845-4cab-8b82-3fcefdec6839?version=1.1.
46. L.F. Walubita, T.P. Nyamuhokya, B. Naik, I. Holleran, S. Dessouky, Sensitivity analysis and validation of the Simple Punching Shear Test (SPST) for screening HMA mixes, Constr. Build. Mater. 169 (2018) 205–214. doi:10.1016/j.conbuildmat.2018.02.198.
47. Z. Hossain, D. Ghosh, M. Zaman, K. Hobson, Use of the Multiple Stress Creep Recovery (MSCR) Test Method to Characterize Polymer-Modified Asphalt Binders, J. Test. Eval. 44 (2016) 507–520. doi:10.1520/jte20140061.
48. A.N.M. Faruk, S.I. Lee, J. Zhang, B. Naik, L.F. Walubita, Measurement of HMA shear resistance potential in the lab : The Simple Punching Shear Test, Constr. Build. Mater. 99 (2015) 62–72. doi:10.1016/j.conbuildmat.2015.09.006.
49. Y.H. Huang, Pavement Analysis and Design, Section ed, 2004.
50. Federal Highway Administration - US Department of Transportation, The Multiple Stress Creep Recovery (MSCR) Procedure, Washington,D.C., 2011.

https://www.fhwa.dot.gov/pavement/materials/pubs/hif11038/hif11038.pdf.

51. L.F. Walubita, L. Fuentes, A. Prakoso, L.M. Rico Pianeta, J.J. Komba, B. Naik, Correlating the HWTT laboratory test data to field rutting performance of in-service highway sections, Constr. Build. Mater. 236 (2020). doi:10.1016/j.conbuildmat.2019.117552.

Tables

Table 1. MSCR Test Result Parameters.

Parameter	Indication of Performance	Analysis Model
$R_{0.1}$ *(%)*	Elastic recovery in linear response to stress range (the greater the value the better)	$= \frac{1}{10}\left\{\sum_{n=1}^{10} \frac{\varepsilon_c^n - \varepsilon_r^n}{\varepsilon_c^n - \varepsilon_0^n}\right\} \times 100$
$R_{3.2}$ *(%)*	Elastic recovery in nonlinear response to stress range. Primary indicator of elastomeric polymer modification. If $R_{3.2} \geq R_{3.2_{min}} = 29.371 * {J_{nr_{3.2}}}^{-0.2633}$, the asphalt-binder has been modified (the greater the value the better)	$= \frac{1}{10}\left\{\sum_{n=1}^{10} \frac{\varepsilon_c^n - \varepsilon_r^n}{\varepsilon_c^n - \varepsilon_0^n}\right\} \times 100$
R_{diff} *(%)*	Sensitivity of polymer modification to stress increases (the greater the value the better)	$= \frac{(R_{0.1} - R_{3.2}) \cdot 100}{R_{0.1}}$
$J_{nr_{0.1}}$*(1/kPa)*	Permanent deformation in linear response to stress range (the lower the value the better)	$= \frac{1}{10}\left\{\sum_{n=1}^{10} \frac{\varepsilon_r^n - \varepsilon_0^n}{0.1}\right\} \times 100$
$J_{nr_{3.2}}$ *(1/kPa)*	Permanent deformation in nonlinear response to stress range. Primary indicator of rutting potential. (the lower the value the better)	$= \frac{1}{10}\left\{\sum_{n=1}^{10} \frac{\varepsilon_r^n - \varepsilon_0^n}{3.2}\right\} \times 100$
$J_{nr_{diff}}$ *(%)*	Sensitivity of shear stress increases (the lower the value the better, $J_{nr_{diff}} \leq 75$ %)	$= \frac{(J_{nr_{3.2}} - J_{nr_{0.1}}) \cdot 100}{J_{nr_{0.1}}}$

Legend: $J_{nr_{0.1}}$ = *Average non-recoverable creep compliance of cycles tested at 0.1 kPa;* $J_{nr_{3.2}}$ = *Average non-recoverable creep compliance of cycles tested at 3.2 kPa;* $J_{nr_{diff}}$ = *Percentage difference in non-recoverable compliance ;* $R_{0.1}$ = *Average recovery of the 10 cycles tested at 0.1 kPa;* $R_{3.2}$ = *Average recovery of the 10 cycles tested at 3.2 kPa;* $R_{3.2_{min}}$ = R_{diff} = *Percentage difference in recovery;* ε_0 = *Initial strain value at the beginning of the creep portion of each cycle;* ε_c = *strain value at the end of the creep portion (that is, after 1.0 s) of each cycle;* ε_r = *strain value at the end of the recovery portion (that is, after 10.0 s) of each cycle.*

Table 2. Alternative HWTT-HMA Rutting Parameters.

Source	Parameter	Analysis Model	Remark
Walubita et al. [5,6,53]	Δ_A Rut_{Δ} $eRL_{(\%)}$	$\Delta_A = \frac{N_d}{2n}[(f(x_0) + 2f(x_1) + 2f(x_2) \ldots + 2f(x_{n-1}) + f(x_n)]$ $Rut_{\Delta} = \frac{\Delta_A}{N_d}$ $eRL_{(\%)} = 1 - 0.08(RD_{PG})$ Where: $f(x_i)$, $f(x_{i+1})$ = *RD* at the left and right end of each trapezoid, respectively; N_d = number of passes to failure; n = number of trapezoids; and RD_{PG}= measured *RD* based on the PG.	N/A ≤8.0 Higher $eRL_{(\%)}$ (higher rutting resistance)
Tsai et al. [54]	*RR*	$RR = \frac{H - RD}{H}$ Where *H*= sample height.	Large *RR* values (high rutting resistance)
Wen et al. [55]	*RRI*	$RRI = N_d * (1 - RD)$	Large *RRI* values (high rutting resistance)

Legend: Δ_A*= Rutting area;* $eRL_{(\%)}$ *= Equivalent remaining rutting life; RR= Rut depth ratio; RRI= Rutting resistance index;* Rut_{Δ}*= Normalized rutting area.*

Table 3. Asphalt-Binders and HMA Volumetric Properties.

#	Mix Type	NMAS	HMA Volumetric Properties			Hwy (Section ID)
			Asphalt-Binder		Aggregates	
1	C_1	18.75 mm (Coarse-Graded)	4.6%	PG 64-22$_{c1}$	+ Limestone/dolomite + 17% RAP (fine) + 3% RAS	US 83 (TxDOT-TTI_00041) (TxDOT-TTI_00081)
2	C_2	18.75 mm	4.8%	PG 64-22$_{c2}$	+ Limestone + 1% lime + 17% RAP (fine) + 3% RAS	SH 21 (TxDOT-TTI_00042)

3	D	(Coarse-Graded) 12.50 mm (Fine-Graded)	5.1%	PG 64-22$_d$	+ Quartzite + 20.1% RAP (10.2% coarse + 9.9% fine)	US 59 (TxDOT-TTI_00001) (TxDOT-TTI_00064)

Legend: Hwy= Highway; NMAS= Nominal maximum aggregate size; RAP= Recycled asphalt pavement; RAS= Recycled asphalt shingles

Table 4. Information of In-Service Test Sections.

#	Section ID (Hwy)	Structure (mm)	District (County) [Date]	Climate Zone (Temp)	Avg. D-ESALs (Gr)	Avg. Spd (SL)
1	TxDOT-TTI_00001 (US 59 [SB])	OL = 50*D+290 E-HMA+400LTB	Atlanta (Panola) [Apr2011]	WC (58.4 °C)	2 380 (2.50%)	69.0 mph (75)
2	TxDOT-TTI_00041 (US 83 [EB])	OL = 50C_1+162.5 E-HMA+200CTB	Laredo (Webb) [Sept2012]	DW (63.1 °C)	1 750 (4.25%)	26.4 mph (35)
3	TxDOT-TTI_00042 (SH 21 [EB])	OL = 62.5C_2+125 E-HMA+300FB	Bryan (Burleson) [Dec2012]	WW (52.8 °C)	1 450 (1.61%)	66.9 mph (75)
4	TxDOT-TTI_00064 (US 59 [NB])	OL = 50D+290 E-HMA+400LTB	Atlanta (Panola)	WC (58.3 °C)	974 (1.84%)	69.3 mph

			[Apr2011]			(75)
5	TxDOT-TTI_00081 (US 83 [WB])	OL = $50C_1$+162.5 E-HMA+200CTB	Laredo (Webb) [Sept2012]	DW (63.1 °C)	1 497 (4.25%)	27.8 mph (35)

*<u>Legend:</u> *The numbers mean the layer thickness (i.e., 290E-HMA = 290 mm thick existing HMA, 400LTB = 400 mm thick lime treated base layer); Avg.= Average; LTB= Lime treated base; CTB= Cement-treated base; D-ESALs= Daily equivalent single axle loads; DW= Dry-warm; EB= Eastbound direction; NB= Northbound direction; SB= Southbound direction; FB= Flexible base; Gr= Growth rate; E-HMA= Existing hot-mix asphalt layer; mph=miles per hour; OL= Overlay; SL= Speed limit; Spd= Speed; Temp.= Temperature; WB= Westbound; WC= Wet-cold; WW= Wet-warm*

Table 5. Asphalt-Binder MSCR Test Results at 58 °C.

Hwy [Section ID]	Asphalt-Binder [HMA mix]	$R_{0.1}$ (%)	$R_{3.2}$ (%)	R_{diff} (%)	$J_{nr_{0.1}}$ (1/kPa)	$J_{nr_{3.2}}$ (1/kPa)	$J_{nr_{diff}}$ (%)
US 83 [TxDOT-TTI_00041] [TxDOT-TTI_00081]	PG 64-22_{c1} [C_1]	39.901	36.608	8.254	0.067	0.068	1.359
SH 21 [TxDOT-TTI_00042]	PG 64-22_{c2} [C_2]	31.802	28.569	10.168	0.112	0.135	21.428
US 59 [TxDOT-TTI_00001] [TxDOT-TTI_00064]	PG 64-22_d [D]	9.626	5.462	43.208	0.727	0.776	6.609

Table 6. Asphalt-Binder MSCR Test Results at 64 °C.

Hwy [**Section ID]**	**Asphalt-Binder** **[HMA mix]**	$R_{0.1}$ *(%)*	$R_{3.2}$ *(%)*	R_{diff} *(%)*	$J_{nr_{0.1}}$ *(1/kPa)*	$J_{nr_{3.2}}$ *(1/kPa)*	$J_{nr_{diff}}$ *(%)*
US 83 [TxDOT-TTI_00041] [TxDOT-TTI_00081]	PG 64-22$_{c1}$ [C_1]	27.591	23.726	14.010	0.179	0.183	2.728
SH 21 [TxDOT-TTI_00042]	PG 64-22$_{c2}$ [C_2]	18.604	15.581	16.258	0.390	0.394	0.962
US 59 [TxDOT-TTI_00001] [TxDOT-TTI_00064]	PG 64-22$_{d}$ [D]	9.183	5.790	36.748	0.722	0.762	5.614

Legend: *HMA= Hot-Mix Asphalt; Hwy= Highway;* $J_{nr_{0.1}}$*= Average non-recoverable creep compliance of cycles tested at 0.1 kPa;* $J_{nr_{3.2}}$*= Average non-recoverable creep compliance of cycles tested at 3.2 kPa;* $J_{nr_{diff}}$ *= Percentage difference in non-recoverable compliance; PG= Performance graded;* $R_{0.1}$ *= Average recovery of the 10 cycles tested at 0.1 kPa;* $R_{3.2}$ *= Average recovery of the 10 cycles tested at 3.2 kPa;* R_{diff} *= Percentage difference in recovery*

Table 7. Laboratory HWTT Results at N_d= 10000.

Hwy **[Section ID]**	**HMA mix** **[Asphalt Binder]**	**AVs** **(CoV)**	***RD*** **(mm)** **[*Slope* (mm/passes)]**	***ΔA*** **(mm-passes)** **[*Rut*Δ (mm)]**	***eRL*** ***(%)***	***RRI*** ***[RR]***
US 83 [TxDOT-TTI_00041] [TxDOT-TTI_00081]	Type C_1 [PG 64-22$_{c1}$]	6.49% (2.40%)	4.05 [4.05E-04]	22 375 [2.24]	67.6	8 382 [0.94]
SH 21 [TxDOT-TTI_00042]	Type C_2 [PG 64-22$_{c2}$]	7.22% (18.19%)	5.36 [5.36E-04]	34 900 [3.49]	57.1	7 856 [0.91]
US 59 [TxDOT-TTI_00001] [TxDOT-TTI_00064]	Type D [PG 64-22$_{d}$]	7.20% (1.98%)	3.40 [3.40E-04]	21 500 [2.15]	72.8	8 640 [0.95]

Table 8. Asphalt-binder and HMA Mix Ranking.

Rank	MSCR @ 58°C		MSCR @ 64°C		HWTT at 50°C, N_d= 10 000			
	$J_{nr_{0.1}}$ (1/kPa)	$J_{nr_{3.2}}$ (1/kPa)	$J_{nr_{0.1}}$ (1/kPa)	$J_{nr_{3.2}}$ (1/kPa)	*RD* (mm) [*Slope* (mm/passes)]	*Rut*$_\Delta$ (mm) [Δ_A (mm-passes)]	*eRL* (%)	*RRI* [*RR*]
1	PG 64-22c_1	PG 64-22c_1	PG 64-22c_1	PG 64-22c_1	D[D]	D[D]	D	D[D]
2	PG 64-22c_2	PG 64-22c_2	PG 64-22c_2	PG 64-22c_2	C_1 [C_1]	C_1 [C_1]	C_1	C_1 [C_1]
3	PG 64-22$_D$	PG 64-22$_D$	PG 64-22$_D$	PG 64-22$_D$	C_2 [C_2]	C_2 [C_2]	C_2	C_2 [C_2]

Table 9. Proposed R^2-based Correlation Strength Scale and Rating Criteria.

Correlation Rating	R^2 Value (%)	Correlation Strength Scale and Color-Coding Scheme	Description
A	$R^2 \geq 60$	Very good	High predictive confidence and accuracy potential
B	$40 \leq R^2 < 60$	Moderate to good	Moderate to reasonable predictive potential
C	$25 \leq R^2 < 40$	Fair	Subjective predictive potential needing cautious interpretation nor acceptance
D	$10 \leq R^2 < 25$	Poor	Uncertainty with low prediction accuracy. User's discretional judgement/decision
E	$R^2 < 10\%$	Very poor	Highly uncertain with very low prediction accuracy. Reject and do not use

Table 10. Correlations (R^2) between R and J_{nr} at 58°C.

Asphalt-Binder MSCR Percent Recovery Parameter	Asphalt-Binder MSCR No-Recoverable Creep Compliance Parameter	R^2 Values				
		Linear (y=ax+b)	Power (y=ax^b)	Exponential (y=ae^{bx})	Logarithmic (y=aLn x +b)	Model with Highest R^2
$R_{0.1}$ (%) @ 58°C	$J_{nr_{0.1}}$ (1/kPa) @ 58°C	97.32%	99.81%	99.45%	99.78%	Power
	$J_{nr_{3.2}}$ (1/kPa) @ 58°C	97.98%	98.94%	99.73%	99.98%	Logarithmic
	$J_{nr_{diff}}$ (%) @ 58°C	1.42%	17.89%	0.08%	25.32%	Logarithmic
$R_{3.2}$ (%) @ 58°C	$J_{nr_{0.1}}$ (1/kPa) @ 58°C	97.57%	99.55%	99.75%	99.85%	Logarithmic
	$J_{nr_{3.2}}$ (1/kPa) @ 58°C	98.20%	98.40%	99.92%	99.96%	Logarithmic
	$J_{nr_{diff}}$ (%) @ 58°C	1.24%	16.10%	0.00%	24.62%	Logarithmic
R_{diff} (%) @ 58°C	$J_{nr_{0.1}}$ (1/kPa) @ 58°C	99.99%	99.50%	99.78%	98.40%	Linear
	$J_{nr_{3.2}}$ (1/kPa) @ 58°C	99.90%	98.31%	99.94%	96.57%	Exponential
	$J_{nr_{diff}}$ (%) @ 58°C	0.30%	15.85%	0.00%	11.97%	Power
Legend: x= Asphalt-Binder ´Percent Recovery Parameter; y= Asphalt-Binder No – Recoverable Creep Compliance Parameter						

Table 11. Correlations (R^2) between R and J_{nr} at 64°C.

Asphalt-Binder MSCR Percent Recovery	Asphalt-Binder MSCR	R^2 Values				
		Linear (y=ax+b)	Power (y=ax^b)	Exponential (y=ae^{bx})	Logarithmic (y=aLn x +b)	

Parameter	No-Recoverable Creep Compliance Parameter					Model with Highest R^2
$R_{0.1}$ (%) @ 64°C	*$J_{nr_{0.1}}$ (1/kPa) @ 64°C*	99.23%	96.81%	99.92%	99.59%	Exponential
	$J_{nr_{3.2}}$ (1/kPa) @ 64°C	98.78%	97.49%	100.00%	99.81%	Exponential
	$J_{nr_{diff}}$ (%) @ 64°C	51.32%	36.41%	62.73%	25.75%	Exponential
$R_{3.2}$ (%) @ 64°C	*$J_{nr_{0.1}}$ (1/kPa) @ 64°C*	99.67%	94.71%	99.35%	99.11%	Linear
	$J_{nr_{3.2}}$ (1/kPa) @ 64°C	99.36%	95.59%	99.67%	99.45%	Exponential
	$J_{nr_{diff}}$ (%) @ 64°C	54.36%	41.53%	67.73%	28.46%	Exponential
R_{diff} (%) @ 64°C	*$J_{nr_{0.1}}$ (1/kPa) @ 64°C*	94.06%	88.02%	95.99%	84.98%	Exponential
	$J_{nr_{3.2}}$ (1/kPa) @ 64°C	95.09%	89.32%	96.84%	86.41%	Exponential
	$J_{nr_{diff}}$ (%) @ 64°C	81.99%	53.61%	78.43%	58.04%	Linear
Legend: x= Asphalt-Binder Percent Recovery Parameter; y= Asphalt-Binder No − Recoverable Creep Compiance Parameter						

Table 12. Correlations (R^2) between MSCR at 58°C and HWTT at N_d=10000.

Asphalt-Binder MSCR Parameter	HMA HWTT Parameter	R^2 Values				
		Linear (y=ax+b)	**Power ($y=ax^b$)**	**Exponential ($y=ae^{bx}$)**	**Logarithmic (y=aLn x +b)**	**Model with Highest R^2**
$R_{0.1}$ (%) @ 58°C	*RD (mm)*	33.75%	49.54%	40.54%	42.53%	Power
	Δ_A (mm-passes)	7.66%	14.55%	8.78%	13.14%	Power
	Rut_Δ (mm)	7.66%	14.55%	8.78%	13.14%	Power
	eRL (%)	33.75%	39.10%	30.49%	42.53%	Logarithmic
	RR	33.75%	42.04%	33.28%	42.53%	Logarithmic

	RRI	33.75%	41.16%	32.44%	42.53%	Logarithmic
	Slope (mm/passes)	33.75%	49.54%	40.54%	42.53%	Power
$R_{3.2}$ *(%) @ 58°C*	*RD (mm)*	34.51%	51.91%	41.33%	44.88%	Power
	Δ_A *(mm-passes)*	8.09%	16.26%	9.24%	14.78%	Power
	Rut_Δ *(mm)*	8.09%	16.26%	9.24%	14.78%	Power
	eRL (%)	34.51%	41.43%	31.24%	44.88%	Logarithmic
	RR	34.51%	44.39%	34.04%	44.88%	Logarithmic
	RRI	34.51%	43.50%	33.19%	44.88%	Logarithmic
	Slope (mm/passes)	34.51%	51.91%	41.33%	44.88%	Power
R_{diff} *(%) @ 58°C*	*RD (mm)*	50.84%	52.26%	57.85%	45.23%	Exponential
	Δ_A *(mm-passes)*	19.26%	16.52%	20.89%	15.03%	Exponential
	Rut_Δ *(mm)*	19.26%	16.52%	20.89%	15.03%	Exponential
	eRL (%)	50.84%	41.78%	47.36%	45.23%	Linear
	RR	50.84%	44.74%	50.34%	45.23%	Linear
	RRI	50.84%	43.85%	49.45%	45.23%	Linear
	Slope (mm/passes)	50.84%	52.26%	57.85%	45.23%	Exponential
$J_{nr_{0.1}}$ *(1/kPa) @ 58°C*	*RD (mm)*	49.89%	45.20%	56.91%	38.26%	Exponential
	Δ_A *(mm-passes)*	18.52%	11.62%	20.13%	10.34%	Exponential
	Rut_Δ *(mm)*	18.52%	11.62%	20.13%	10.34%	Exponential
	eRL (%)	49.89%	34.90%	46.41%	38.26%	Linear
	RR	49.89%	37.78%	49.40%	38.26%	Linear
	RRI	49.89%	36.91%	48.50%	38.26%	Linear
	Slope (mm/passes)	49.89%	45.20%	56.91%	38.26%	Exponential
$J_{nr_{3.2}}$ *(1/kPa) @ 58°C*	*RD (mm)*	47.70%	39.33%	54.73%	32.58%	Exponential
	Δ_A *(mm-passes)*	16.84%	8.09%	18.39%	7.01%	Exponential
	Rut_Δ *(mm)*	16.84%	8.09%	18.39%	7.01%	Exponential
	eRL (%)	47.70%	29.36%	44.22%	32.58%	Linear
	RR	47.70%	32.11%	47.20%	32.58%	Linear
	RRI	47.70%	31.28%	46.31%	32.58%	Linear
	Slope (mm/passes)	47.70%	39.33%	54.73%	32.58%	Exponential

$J_{nr_{diff}}$ *(%) @ 58°C*	*RD (mm)*	54.59%	11.97%	47.56%	16.90%	Linear
	Δ_A (mm-passes)	84.84%	45.75%	83.35%	47.78%	Linear
	Rut_Δ (mm)	84.84%	45.75%	83.35%	47.78%	Linear
	eRL (%)	54.59%	19.59%	58.05%	16.90%	Exponential
	RR	54.59%	17.28%	55.09%	16.90%	Exponential
	RRI	54.59%	17.96%	55.98%	16.90%	Exponential
	Slope (mm/passes)	54.59%	11.97%	47.56%	16.90%	Linear
<u>*Legend:*</u> x= Asphalt-Binder MSCR Parameter; y=HMA HWTT rutting Parameter						

Table 13. Correlation (R^2) between MSCR at 64°C and HWTT at N_d=10000.

Asphalt-Binder MSCR Parameter	HWTT Parameter	R^2 Values				
		Linear (y=ax+b)	**Power ($y=ax^b$)**	**Exponential ($y=ae^{bx}$)**	**Logarithmic (y=aLn x +b)**	**Model with Highest R^2**
$R_{0.1}$ *(%) @ 64°C*	*RD (mm)*	17.03%	32.94%	22.63%	26.52%	Power
	Δ_A (mm-passes)	0.74%	4.84%	1.13%	4.00%	Power
	Rut_Δ (mm)	0.74%	4.84%	1.13%	4.00%	Power
	eRL (%)	17.03%	23.50%	14.49%	26.52%	Logarithmic
	RR	17.03%	26.08%	16.66%	26.52%	Logarithmic
	RRI	17.03%	25.30%	16.00%	26.52%	Logarithmic
	Slope (mm/passes)	17.03%	32.94%	22.63%	26.52%	Power
$R_{3.2}$ *(%) @ 64°C*	*RD (mm)*	19.38%	37.96%	25.23%	31.27%	Power
	Δ_A (mm-passes)	1.35%	7.34%	1.86%	6.31%	Power
	Rut_Δ (mm)	1.35%	7.34%	1.86%	6.31%	Power
	eRL (%)	19.38%	28.09%	16.70%	31.27%	Logarithmic

	RR	19.38%	30.81%	18.99%	31.27%	Logarithmic
	RRI	19.38%	29.99%	18.29%	31.27%	Logarithmic
	Slope (mm/passes)	19.38%	37.96%	25.23%	31.27%	Power
R_{diff} *(%) @ 64°C*	*RD (mm)*	47.39%	49.97%	54.42%	42.95%	Exponential
	Δ_A *(mm-passes)*	16.61%	14.85%	18.16%	13.43%	Exponential
	Rut_Δ *(mm)*	16.61%	14.85%	18.16%	13.43%	Exponential
	eRL (%)	47.39%	39.52%	43.92%	42.95%	Linear
	RR	47.39%	42.46%	46.89%	42.95%	Linear
	RRI	47.39%	41.57%	46.00%	42.95%	Linear
	Slope (mm/passes)	47.39%	49.97%	54.42%	42.95%	Exponential
$J_{nr_{0.1}}$ *(1/kPa) @ 64°C*	*RD (mm)*	24.09%	17.51%	30.34%	12.49%	Exponential
	Δ_A *(mm-passes)*	2.98%	0.18%	3.71%	0.05%	Exponential
	Rut_Δ *(mm)*	2.98%	0.18%	3.71%	0.05%	Exponential
	eRL (%)	24.09%	10.28%	21.17%	12.49%	Linear
	RR	24.09%	12.17%	23.66%	12.49%	Linear
	RRI	24.09%	11.59%	22.91%	12.49%	Linear
	Slope (mm/passes)	24.09%	17.51%	30.34%	12.49%	Exponential
$J_{nr_{3.2}}$ *(1/kPa) @ 64°C*	*RD (mm)*	26.07%	19.09%	32.47%	13.88%	Exponential
	Δ_A *(mm-passes)*	3.81%	0.39%	4.63%	0.18%	Exponential
	Rut_Δ *(mm)*	3.81%	0.39%	4.63%	0.18%	Exponential
	eRL (%)	26.07%	11.56%	23.07%	13.88%	Linear
	RR	26.07%	13.54%	25.64%	13.88%	Linear
	RRI	26.07%	12.93%	24.86%	13.88%	Linear
	Slope (mm/passes)	26.07%	19.09%	32.47%	13.88%	Exponential
$J_{nr_{diff}}$ *(%) @ 64°C*	*RD (mm)*	86.71%	99.87%	91.11%	98.86%	Power
	Δ_A *(mm-passes)*	57.25%	82.93%	59.26%	81.37%	Power
	Rut_Δ *(mm)*	57.25%	82.93%	59.26%	81.37%	Power
	eRL (%)	86.71%	98.01%	84.25%	98.86%	Logarithmic
	RR	86.71%	98.75%	86.37%	98.86%	Logarithmic
	RRI	86.71%	98.55%	85.75%	98.86%	Logarithmic

	Slope (mm/passes)	86.71%	99.87%	91.11%	98.86%	Power
Legend: x= Asphalt-Binder MSCR Parameter; y=HMA HWTT Rutting Parameter						

Table 14. Correlations (R^2) between MSCR at 58°C and HMA Field Performance.

MSCR Parameters	**Field Rutting Parameters**	**R^2 Values**				
		Linear (y=ax+b)	**Power ($y=ax^b$)**	**Exponential ($y=ae^{bx}$)**	**Logarithmic (y=aLn x+b)**	**Model with Highest R^2**
$R_{0.1}$ *(%) @ 58°C*	*RD 6.23 years(mm)*	23.55%	33.56%	26.78%	30.49%	Power
	RD 2.68 MESALs (mm)	5.64%	8.44%	4.65%	10.00%	Logarithmic
	Slope A (mm/year)	9.65%	11.40%	7.66%	14.12%	Logarithmic
	Slope B (mm/ MESALs)	0.28%	2.08%	0.66%	1.52%	Power
$R_{3.2}$ *(%) @ 58°C*	*RD 6.23 years(mm)*	24.14%	35.37%	27.37%	32.37%	Power
	RD 2.68 MESALs (mm)	5.98%	9.59%	4.95%	11.32%	Logarithmic
	Slope A (mm/year)	10.02%	12.48%	7.96%	15.39%	Logarithmic
	Slope B (mm/ MESALs)	0.35%	2.58%	0.75%	2.01%	Power
R_{diff} *(%) @ 58°C*	*RD 6.23 years(mm)*	37.18%	35.63%	39.94%	32.65%	Exponential
	RD 2.68 MESALs (mm)	14.93%	9.77%	12.76%	11.52%	Linear
	Slope A (mm/year)	18.74%	12.64%	15.32%	15.58%	Linear
	Slope B (mm/MESALs)	3.52%	2.65%	4.05%	2.09%	Exponential
$J_{nr_{0.1}}$ *(1/kPa) @ 58°C*	*RD 6.23 years(mm)*	36.41%	30.27%	39.21%	27.10%	Exponential
	RD 2.68 MESALs (mm)	14.33%	6.50%	12.23%	7.77%	Linear
	Slope A (mm/year)	18.19%	9.53%	14.86%	11.89%	Linear
	Slope B (mm/MESALs)	3.25%	1.30%	3.79%	0.80%	Exponential
$J_{nr_{3.2}}$ *(1/kPa) @ 58°C*	*RD 6.23 years(mm)*	34.63%	25.88%	37.53%	22.63%	Exponential
	RD 2.68 MESALs (mm)	12.98%	4.22%	11.05%	5.13%	Linear
	Slope A (mm/year)	16.95%	7.19%	13.80%	9.09%	Linear

	Slope B (mm/MESALs)	2.67%	0.52%	3.23%	0.18%	Exponential
$J_{nr_{diff}}$ *(%) @ 58°C*	*RD 6.23 years(mm)*	48.75%	12.26%	40.92%	17.13%	Linear
	RD 2.68 MESALs (mm)	71.62%	37.72%	64.73%	41.19%	Linear
	Slope A (mm/year)	47.71%	20.66%	42.15%	22.77%	Linear
	Slope B (mm/MESALs)	59.63%	31.85%	47.01%	42.39%	Linear
Legend: x= Asphalt-Binder MSCR Parameter; y= Field Rutting HMA- Layer Parameter						

Table 15. Correlation (R^2) between MSCR at 64°C and HMA Field Performance.

MSCR Parameters	**Field Rutting Parameters**	**R^2 Values**				
		Linear ($y=ax+b$)	**Power ($y=ax^b$)**	**Exponential ($y=ae^{bx}$)**	**Logarithmic ($y=aLn\ x+b$)**	**Model with Highest R^2**
$R_{0.1}$ *(%) @ 64°C*	*RD 6.23 years(mm)*	10.82%	21.18%	13.78%	17.95%	Power
	RD 2.68 MESALs (mm)	0.39%	2.23%	0.25%	2.80%	Logarithmic
	Slope A (mm/year)	2.66%	4.91%	1.92%	6.35%	Logarithmic
	Slope B (mm/MESALs)	1.00%	0.07%	0.31%	0.01%	Linear
$R_{3.2}$ *(%) @ 64°C*	*RD 6.23 years(mm)*	12.56%	24.87%	15.62%	21.62%	Power
	RD 2.68 MESALs (mm)	0.82%	3.75%	0.58%	4.59%	Logarithmic
	Slope A (mm/year)	3.49%	6.68%	2.59%	8.48%	Logarithmic
	Slope B (mm/MESALs)	0.58%	0.39%	0.12%	0.10%	Linear
R_{diff} *(%) @ 64°C*	*RD 6.23 years(mm)*	**34.38%**	**33.88%**	**37.29%**	**30.82%**	Exponential
	RD 2.68 MESALs (mm)	12.79%	8.64%	10.88%	10.23%	Linear
	Slope A (mm/year)	16.77%	11.59%	13.65%	14.34%	Linear
	Slope B (mm/MESALs)	2.59%	2.16%	3.16%	1.60%	Exponential
$J_{nr_{0.1}}$ *(1/kPa) @ 64°C*	*RD 6.23 years(mm)*	16.10%	10.22%	19.29%	7.53%	Exponential
	RD 2.68 MESALs (mm)	2.02%	0.00%	1.57%	0.00%	Linear
	Slope A (mm/year)	5.32%	0.84%	4.07%	1.28%	Linear
	Slope B (mm/MESALs)	0.10%	1.01%	0.00%	2.24%	Logarithmic
	RD 6.23 years(mm)	17.61%	11.31%	20.83%	8.53%	Exponential

$J_{nr_{3.2}}$ *(1/kPa) @ 64°C*	*RD 2.68 MESALs (mm)*	2.65%	0.02%	2.10%	0.05%	Linear
	Slope A (mm/year)	6.16%	1.14%	4.76%	1.67%	Linear
	Slope B (mm/MESALs)	0.02%	0.74%	0.05%	1.79%	Logarithmic
$J_{nr_{diff}}$ *(%) @ 64°C*	*RD 6.23 years(mm)*	**67.63%**	**76.01%**	**67.13%**	**79.48%**	Logarithmic
	RD 2.68 MESALs (mm)	46.25%	59.04%	40.64%	**66.61%**	Logarithmic
	Slope A (mm/year)	43.64%	48.63%	**36.85%**	56.89%	Logarithmic
	Slope B (mm/ MESALs)	22.31%	**33.33%**	20.29%	**38.56%**	Logarithmic
Legend: x= Asphalt-Binder MSCR Parameter; y= Field Rutting HMA- Layer Parameter						

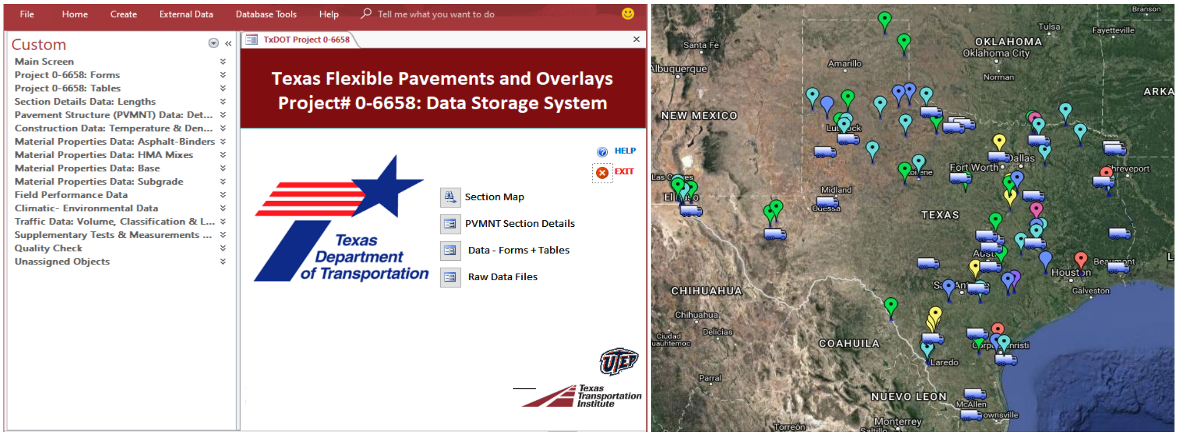

Fig. 1. The DSS Interface Screen and Test Section Locations.

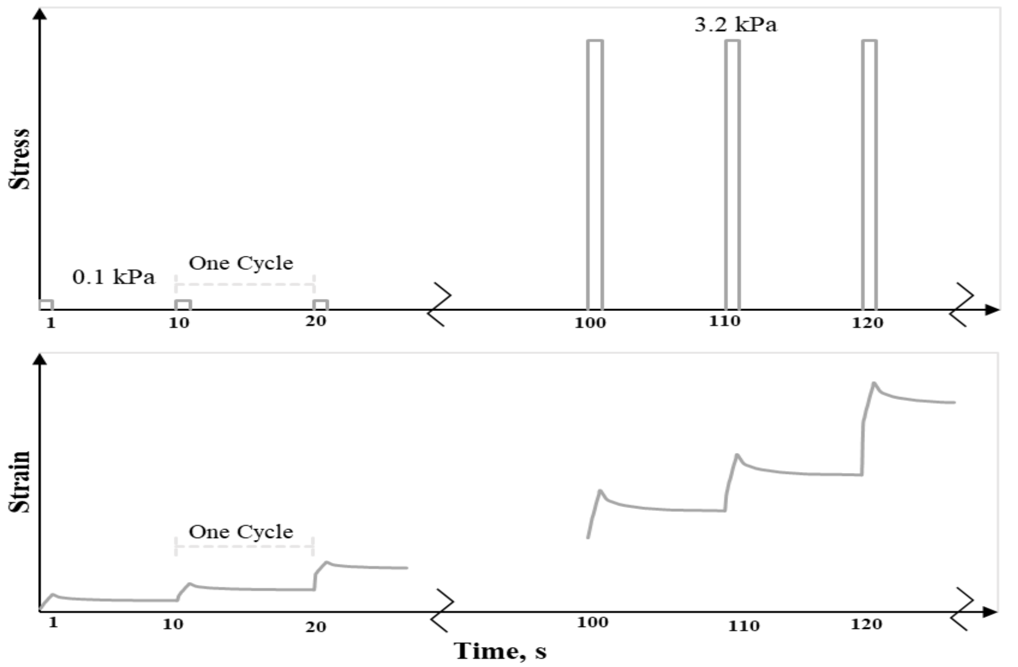

Fig. 2. Schematic of Three MSCR Load Cycles at Two Stress Levels.

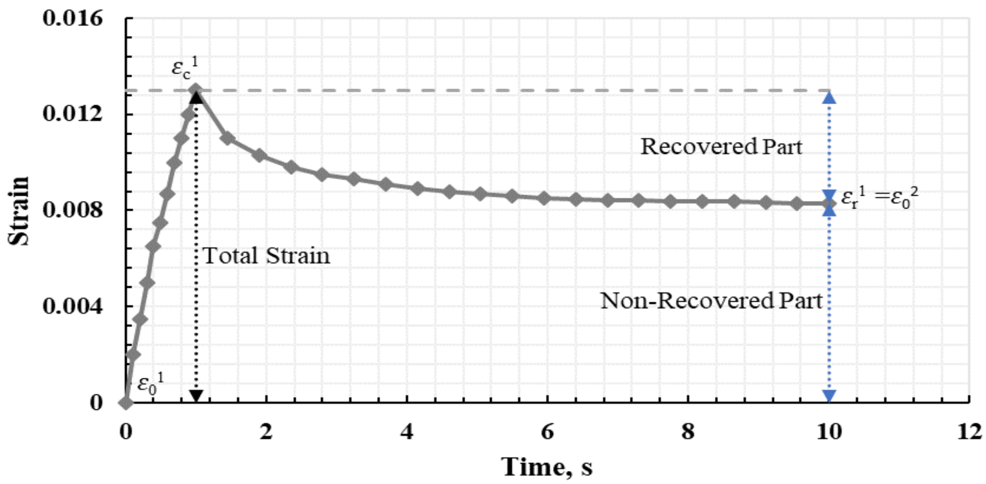

Fig. 3. Example MSCR Creep Strain Response as a Function of Time.

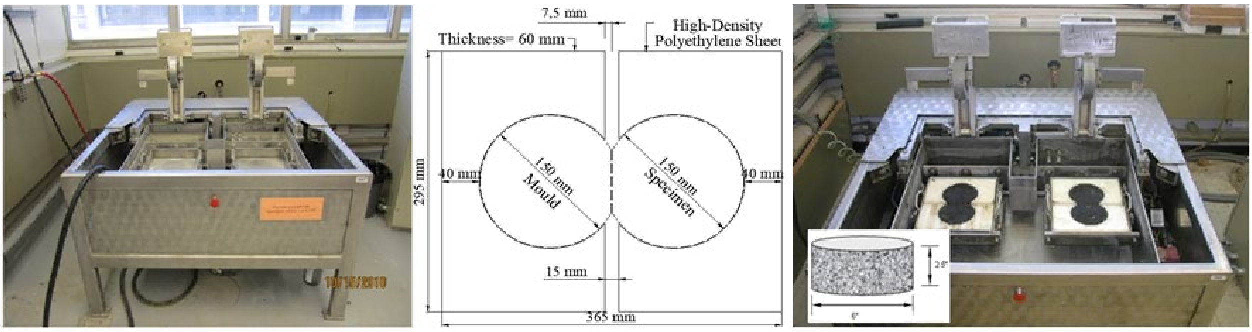

Fig. 4. The HWTT Device.

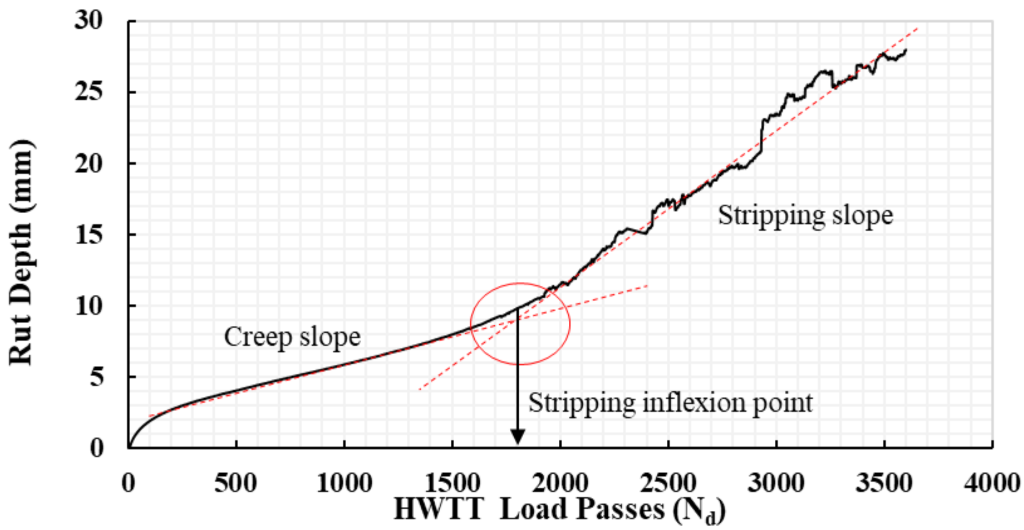

Fig. 5. Typical HWTT Rutting Response-Curve.

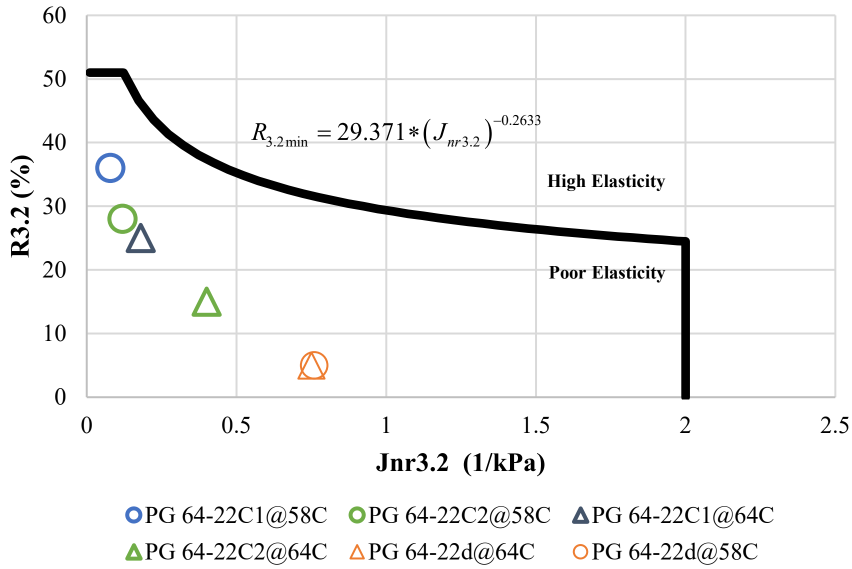

Fig. 6. Standard MSCR Curve to Assess Asphalt-Binder Elastic Response.

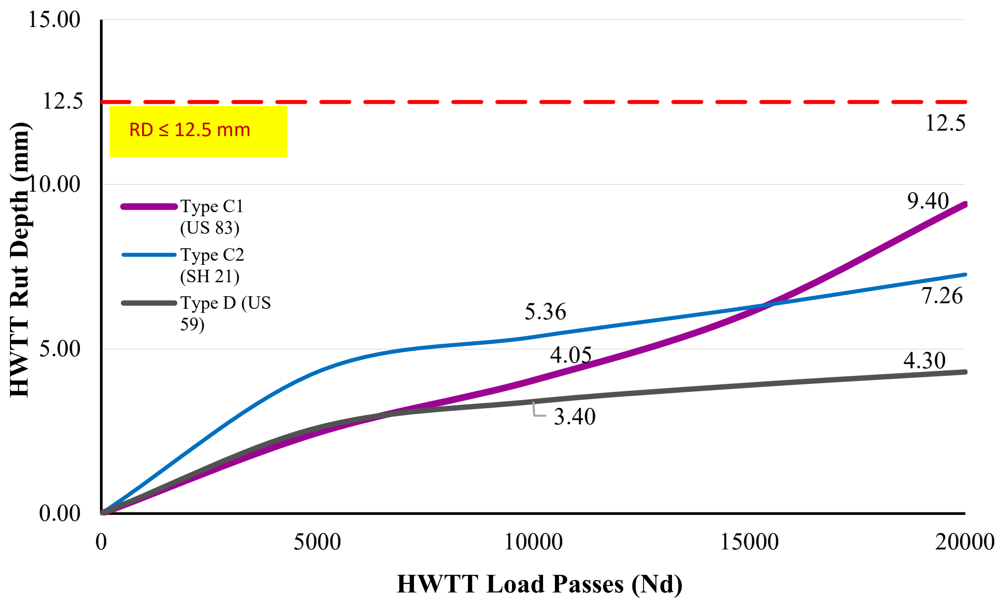

Fig. 7. HWTT Rutting Response-Curves.

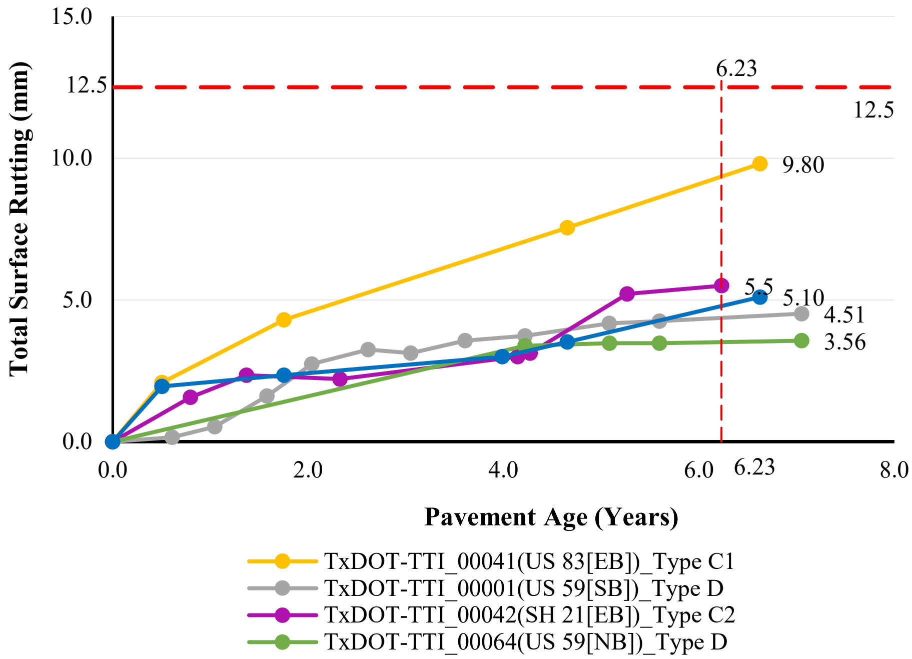

Fig. 8. Total Rut Depth with Pavement Age.

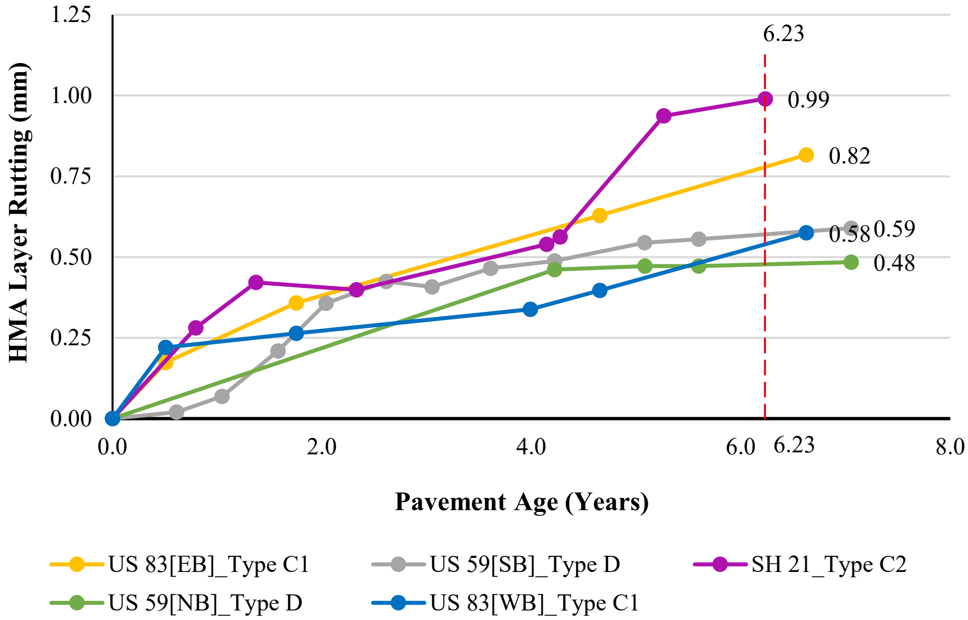

Fig. 9. HMA Layer RD with Pavement Age.

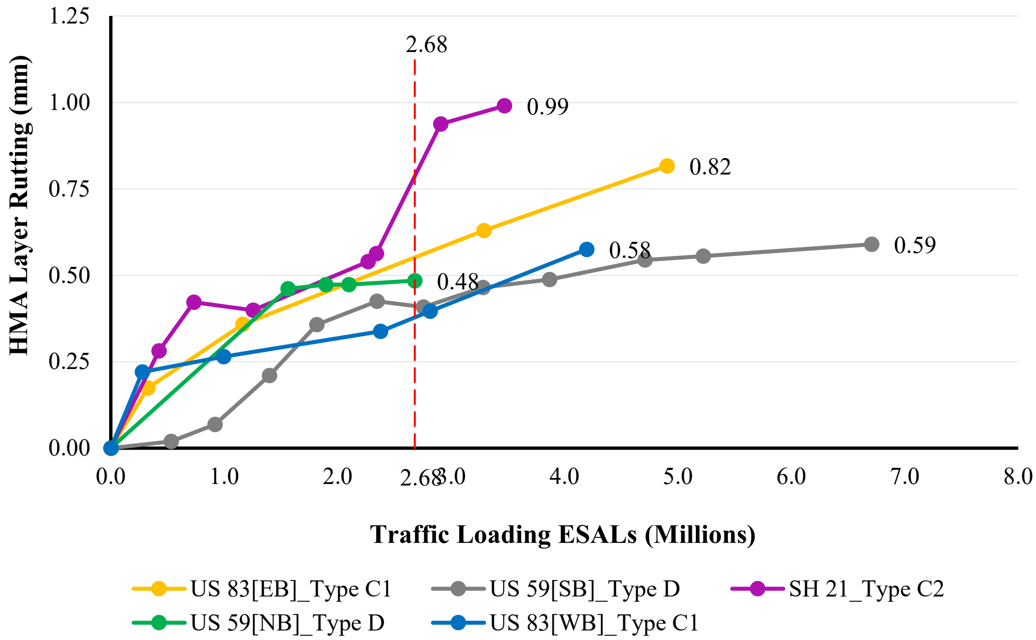

Fig. 10. HMA Layer RD with Traffic Level.

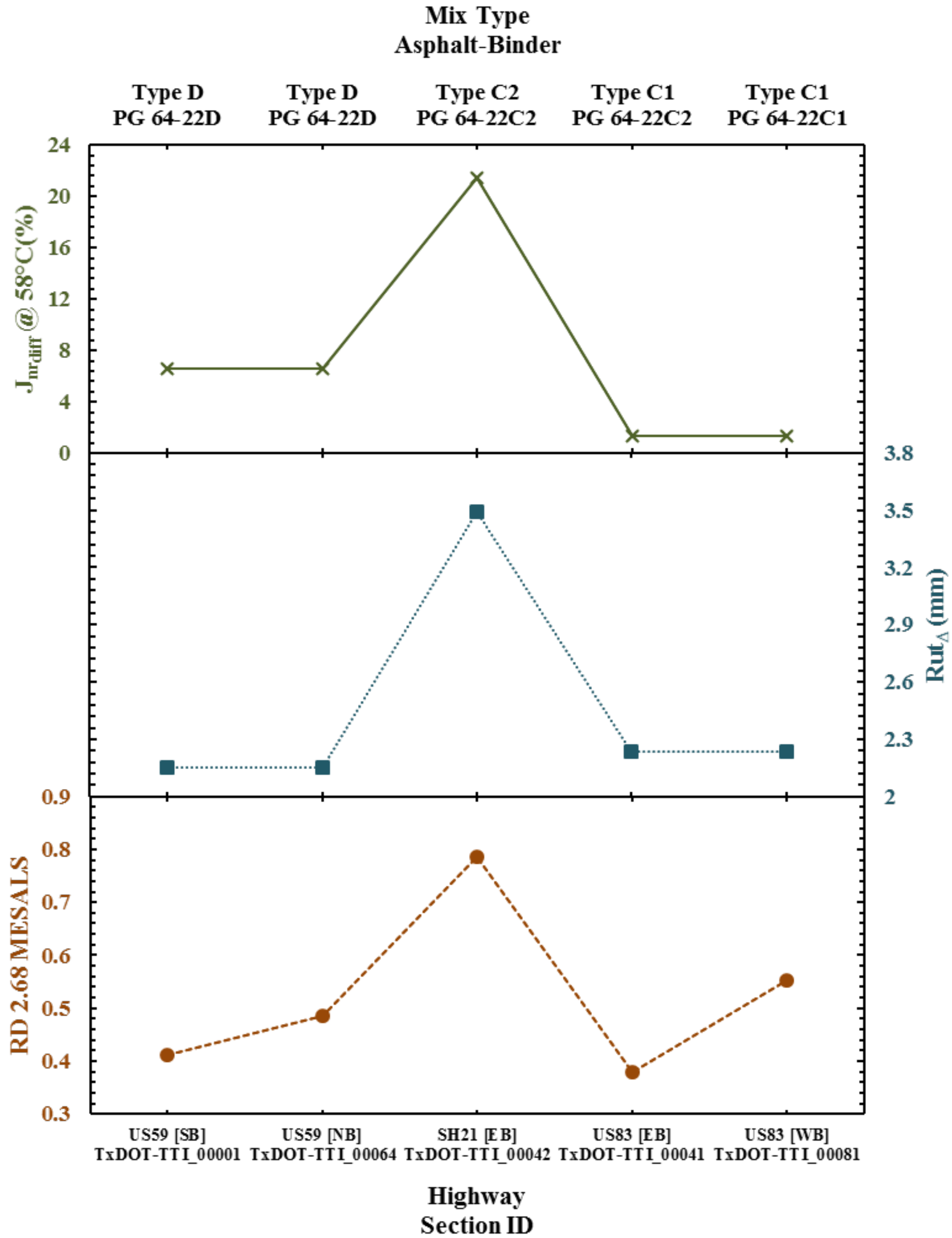
Mix Type
Asphalt-Binder
Type D
PG 64-22D
Type D
PG 64-22D
Type C2
PG 64-22C2
Type C1
PG 64-22C2
Type C1
PG 64-22C1
$J_{nr_{diff}}$ @ 58°C(%)
24
20
16
12
8
4
0
3.8
3.5
3.2
2.9
2.6
2.3
2
Rut_Δ (mm)
0.9
0.8
0.7
0.6
0.5
0.4
0.3
RD 2.68 MESALS
US59 [SB]
TxDOT-TTI_00001
US59 [NB]
TxDOT-TTI_00064
SH21 [EB]
TxDOT-TTI_00042
US83 [EB]
TxDOT-TTI_00041
US83 [WB]
TxDOT-TTI_00081
Highway
Section ID

(a)

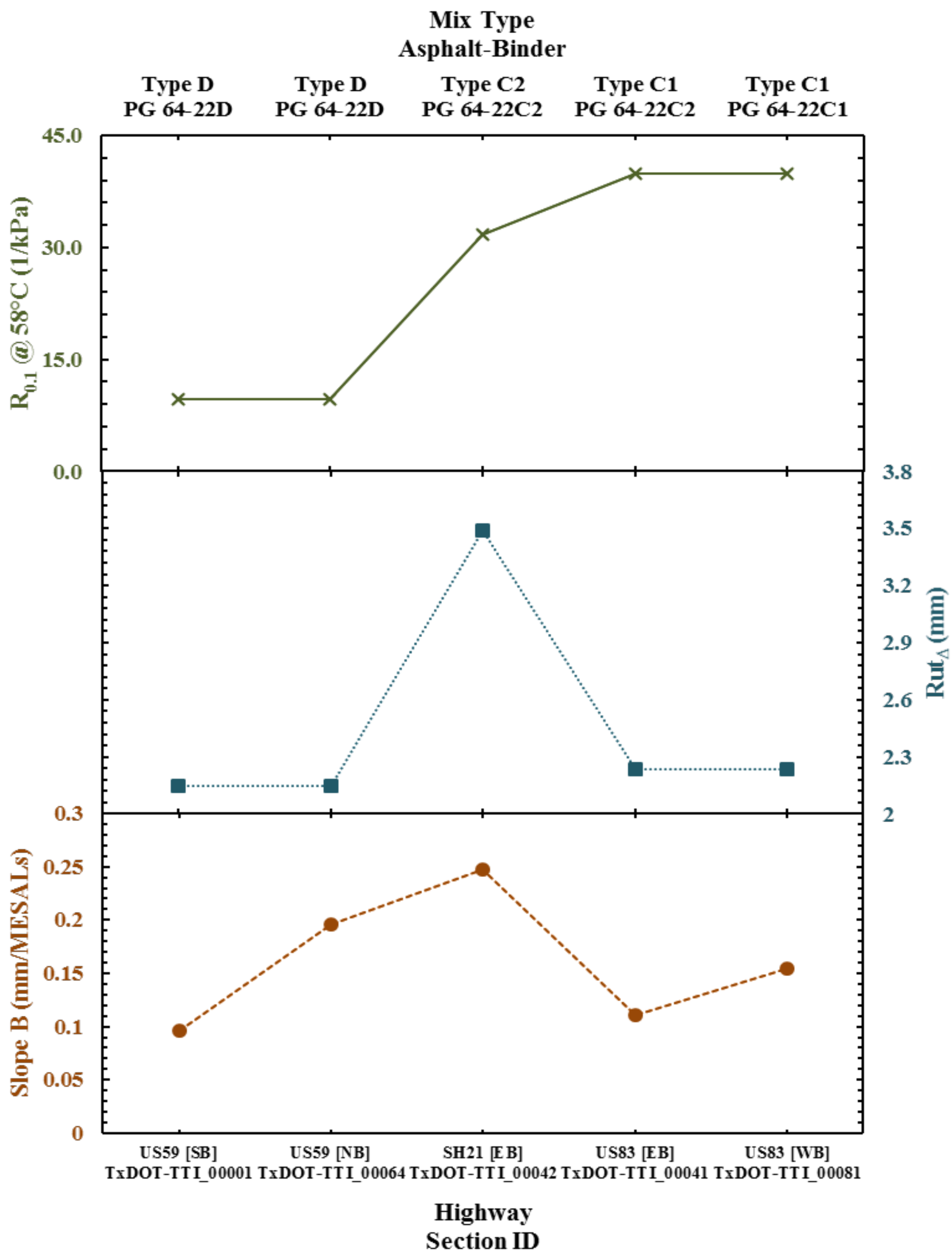

(b)

Fig. 11. MSCR-HWTT-Field Correlations: (a) Good to Very Good, (b) Very Poor to Fair.

Fig. 1. The DSS Interface Screen and Test Section Locations.

Fig. 2. Schematic of Three MSCR Load Cycles at Two Stress Levels.

Fig. 3. Example MSCR Creep Strain Response as a Function of Time.

Fig. 4. The HWTT Device.

Fig. 5. Typical HWTT Rutting Response-Curve.

Fig. 6. Standard MSCR Curve to Assess Asphalt-Binder Elastic Response.

Fig. 7. HWTT Rutting Response-Curves.

Fig. 8. Total Rut Depth with Pavement Age.

Fig. 9. HMA Layer RD with Pavement Age.

Fig. 10. HMA Layer RD with Traffic Level.

Fig. 11. MSCR-HWTT-Field Correlations: (a) Good to Very Good, (b) Very Poor to Fair.